EVALUATION OF LOCAL STRESS-STRAIN METHODS

A Thesis

Submitted to the faculty of Graduate Studies and Research

In Partial Fulfillment of the Requirements

for the Degree of

Masters of Applied Science

in Industrial Systems Engineering

University of Regina

by

Prabhaker Rao Navathe

Regina, Saskatchewan

April, 1997

Abstract

Notch-tip strains and fatigue crack initiation life in an SAE compact tension keyhole specimen have been estimated under plane stress and plane strain conditions using three local stress-strain methods - Neuber's rule, Improved Neuber's rule and Equivalent Strain-Energy Density method. The estimates obtained are compared with the experimental results from the literature to evaluate the capabilities of these local stress-strain methods.

It was found that Neuber's rule overestimated the notch-tip strains and grossly underestimated the fatigue crack initiation life. The energy approach was found to be the best. Improved Neuber's rule estimated strains as well as fatigue lives far better than Neuber's rule. The strain estimates were found to be within a range of 10 to 12% and the fatigue life estimates were within 15 to 20% of the corresponding estimates by energy approach.

It was concluded that the improved Neuber's rule can effectively replace conventional Neuber's rule and, owing to its simpler calculations, can also be used in place of the intricate energy approach.

Acknowledgments

I would like to acknowledge my supervisor, Dr. W.B.H. Cooke, for his invaluable guidance, encouragement and advice during the various stages of research and thesis preparation. The financial support provided by the Faculty of Graduate Studies and the Faculty of Engineering, at the University of Regina, in the form of assistantships and scholarships, is gratefully acknowledged.

I wish to thank Dr. S.D. Bhole for all his help and support during my study at the university.

I would like to thank for the support and company provided by all my friends, which made my stay in Regina a pleasant and memorable one. I would like to acknowledge Shiv for helping me with the computer code.

Finally, without the encouragement and support of my brother Sudhakar, this stage would have remained unattainable. I dedicate this thesis to my family.

Nomenclature

A	Cross sectional area
b	Fatigue strength exponent
c	Fatigue ductility exponent
C_p	Plastic-zone correction factor
E	Young's modulus -- Plane stress
E^*	Young's modulus -- Plane strain
I	Moment of inertia
K	Monotonic strength coefficient
K'	Cyclic strength coefficient -- plane stress
K^*	Cyclic strength coefficient -- plane strain
K_t	Theoretical elastic stress-concentration factor
K_f	Fatigue notch factor
K_σ	Elastic-plastic stress-concentration factor
K_ε	Elastic-plastic strain-concentration factor
M	Moment about the neutral axis
n	Monotonic strain-hardening exponent
n'	Cyclic strain-hardening exponent - plane stress
n^*	Cyclic strain-hardening exponent - plane strain
N	Number of cycles to crack initiation
$2N$	Number of reversals to crack initiation
P	Applied load
R	Stress ratio

S_a	Nominal stress
S_{max}	Maximum nominal stress
S_{min}	Minimum nominal stress
S_m	Mean stress
ΔS	Nominal (average) net section stress range
W_e	Notch-tip strain-energy density due to the theoretical elastic stress
W_p	Notch-tip strain-energy density due to the elastic-plastic stress
z	Distance from the neutral axis
ε	Notch-tip strain
ε_a , E_a	Notch-tip strain amplitude -- plane stress
ε^*_a	Notch-tip strain amplitude -- plane strain
e	Elastic notch-tip strain
ε'_f	Fatigue ductility coefficient
ε_t	Total strain component
ε_e	Elastic strain component
ε_p	Plastic strain component
$\Delta\varepsilon$	Notch-tip strain range
σ	Notch-tip stress
σ_a	Notch-tip stress amplitude -- plane stress
σ^*_a	Notch-tip stress amplitude -- plane strain
σ'_f	Fatigue strength coefficient
σ_m	Notch-tip mean stress
σ_{ys}	Yield strength -- plane stress
σ^*_{ys}	Yield strength -- plane strain
$\Delta\sigma$	Notch-tip stress range
υ	Poisson's ratio
ρ	Notch-tip radius
r_p	Plastic zone size -- plane stress
r^*_p	Plastic zone size -- plane strain

Table of Contents

List of Tables

List of Figures

Chapter One

INTRODUCTION

1.1 INTRODUCTION

Since the advent of the steam engine and mechanical transport, failures of moving parts carrying a repeatedly applied load have become a common occurrence. These are fatigue failures and are usually located at a change in section, such as a hole, a change in shaft diameter, a groove, a keyway or even a tool mark. The change in section gives rise to a stress raiser or stress concentration which is known as fatigue critical locations. The number of failures in service due to fatigue has continued to increase with the ever increasing demand for more efficient and economic components such as, higher operating speeds and minimum weight design. Today, fatigue is by far the most common cause of failure for load-carrying metallic components.

Every component has a finite fatigue life though the designs are aimed at making them last forever. Usually the number of loading cycles to failure is treated as a measure of fatigue life. To avoid catastrophic failures, there is a definite need to estimate the fatigue

life in a component or structure. It is highly essential, especially in existing structures where the service requirements have been altered at a later date. Fatigue life estimates can aid in setting up maintenance schedules under a rational premise, such that timely corrective action can be taken. Further, fatigue life of a critical component can dictate the life of the entire assembly. It is highly desirable to build all the parts in an assembly with an approximately equal life, such that only a small amount of life (of the remaining parts) is lost when the assembly as a whole is ready to be discarded. This concept was first conceived by Henry Ford. Therefore fatigue life estimates have a significant impact on the economics of the industry by contributing to the efforts towards avoiding catastrophic failures.

Aluminum alloys, because of their high strength to weight ratio, are extensively used in the manufacture of aircraft structures. There are certain difficulties in welding these alloys and the only means of joining [up to date] is the use of rivets. Holes, which come as part of riveting operations, are stress raisers and create potential zones for fatigue cracks initiation. Similar problem areas are common in the auto industry where sheet metal is extensively used in the manufacture of body panels, doors and hoods. New designs call for modification in their profiles and their supporting structure. Though efforts are made during the design phase to avoid critical fatigue locations, all new designs must nevertheless be subjected to fatigue tests under simulated road loading.

The three main factors in estimating fatigue life are:

1. Material properties

2. Geometric properties and

3. Local stress-strain history

Material properties consist of cyclic stress-strain response and strain-life data. These are obtained by subjecting smooth specimens to strain controlled fatigue tests. Large collections of such data have been generated by numerous researchers over the past three decades.

The local stress-strain history, particularly in the vicinity of the stress raiser, is of great significance. It is well established that the notch-tip strain is the critical factor in crack initiation. Fatigue life can be estimated from the Coffin-Manson [1], [2] relation, provided the strains at the fatigue critical location are available. Further, it was verified by Wetzel [3] that the fatigue crack initiation life of a notched component is equal to the fatigue life of a plain specimen if the notch-tip of the component and the unnotched (smooth) specimen both experience the same strain history. This postulate has been found very useful, particularly in case of complex notch geometries.

It is apparent that knowing the local notch-tip strains are essential in estimating fatigue life. The accuracy of these calculations depends on the approach adopted and has a considerable influence on fatigue life estimates. Different approaches for calculating local stresses and strains were proposed and constant efforts were made to improve these methods, such as:

1. Strain Measurement using strain gauges and other sophisticated instrumentation

2. Finite Element or Boundary Integral methods

3. Local stress-strain methods

Experimental strain measurement could be effective in simple notches but the present instrumentation technology is not good enough to accommodate the strain measurement in complex notch geometries.

Finite element (FE) or boundary integral methods are quite effective and accurate, irrespective of the complexity of the notch geometry. But the fatigue life estimation involves lengthy cyclic loading histories where FE methods might prove to be costly and complex. Hence, the local stress-strain methods have gained momentum over the last two decades and evolved as an effective technique in the estimation of notch-tip stress-strains.

Taking these aspects into consideration, a comparative study of the frequently used local stress-strain methods has been undertaken, in this thesis. This will not only lead to a better understanding of these methods but will also contribute towards making efficient estimates of fatigue crack initiation life.

1.2 Objective

The main objective of the present work is:

To evaluate the capabilities of three local stress-strain methods and to study how good the notch-tip strain and the fatigue life estimates obtained using the improved Neuber's rule

are when compared to Neuber's rule and the Equivalent Strain-Energy Density (ESED) method, so as to suggest any possible revision of the practices in today's industry.

1.3 Organization of thesis

Chapter Two deals with some of the basic concepts in fatigue behavior with a focus on understanding cyclic loading and the material stress-strain curve. It is followed by a more detailed background on the cause of fatigue failures and the evolution of analytical methods. The SAE keyhole specimen adopted in the present evaluation, along with the applied loading conditions, are described.

In Chapter Three, the three local stress-strain methods are discussed. Fatigue life estimation from the calculated notch-tip strains is detailed in this chapter.

The results obtained from the local stress-strain methods are presented in Chapter Four. These are then compared with the experimental results obtained from the literature. A discussion on the significance of the comparative evaluation is then presented.

Chapter Five provides the main conclusions of this work. The scope for further research based on the work done in this thesis is then examined.

Appendix A lists the complete computer code in 'C' which is used to do the various computations involved in the estimation of notch-tip strains and fatigue crack initiation

life. A sample calculation is presented in appendix B. Relation between the applied load (P) and the nominal stress (S_a) is derived in appendix C.

Chapter Two

BASIC CONCEPTS

2.1 Fatigue

Fatigue in materials is a common problem that affects virtually everything that moves and may fail in fatigue if subjected to cyclically imposed forces or deformations. There are innumerable problem areas. Automobiles fatigue from rough roads, airplane wings flutter in flight, bridges deflect under each passing vehicle and nuclear reactors are damaged by cyclic temperature changes. The subject of fatigue is complex and can be studied in many different ways. From the engineering point of view the approach based on an analysis of stress and strain is one of the most important.

2.2 Cyclic Loading Conditions

Cyclic-loading conditions are frequently imposed on materials in service and this is one of the important aspects in understanding stress and strain in materials fatigue. Figure 2.1 shows the notation usually followed under the simplest imposed conditions, in which the loading is harmonically reversed and repeated. Stress or strain is used as a loading function since these parameters best describe the material's behavior. One of the two

quantities is controlled in such a way that the peaks are constant from cycle to cycle, and the other quantity is allowed to vary according to the character of the material. Lower and upper peaks of the loading play a vital role in fatigue problems.

Definitions of alternating, mean, maximum, minimum, and range of stress are shown in figure 2.1. The algebraic relationships among these terms are:

Nominal stress, $S_a = \frac{S_{max} - S_{min}}{2}$

Mean Stress, $S_m = \frac{S_{max} + S_{min}}{2}$

Maximum nominal stress, $S_{max} = S_m + S_a$

Minimum nominal stress, $S_{min} = S_m - S_a$

Stress ratio, $R = \frac{S_{min}}{S_{max}}$

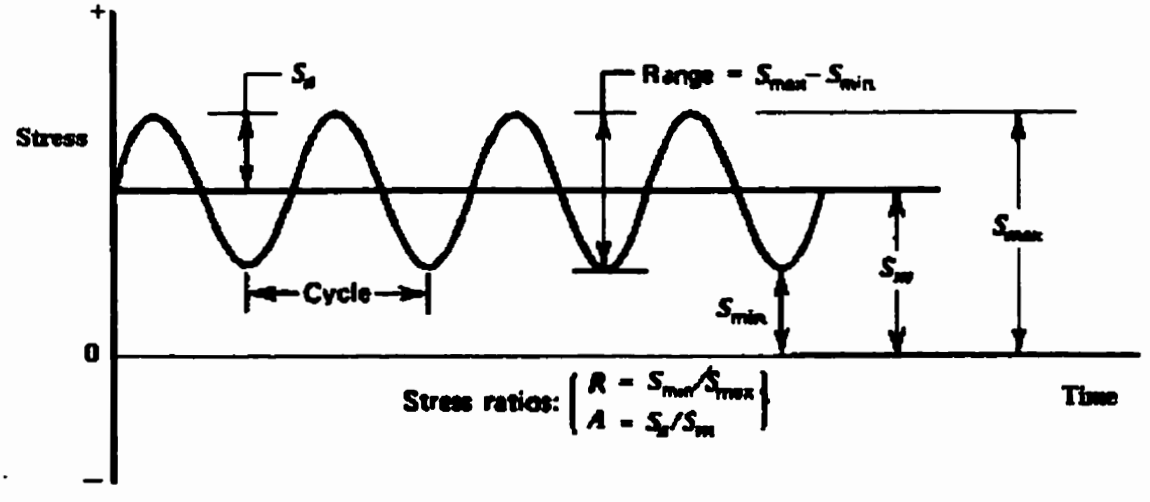

Figure 2.1 Cyclic Loading

When a material is cyclically loaded within the elastic region, stress and strain are linearly related to each other by the elastic modulus and they cycle about a straight line. Stress-strain responses become more complex when the loading exceeds the elastic limit, thereby causing inelastic deformation. When the material is cyclically loaded *beyond* its elastic limit, say to point A in figure 2.2, and unloaded, the material stress-strain curve does not retrace its path. It follows a straight line with a slope equal to that of elastic modulus and the load is reversed into compression (point B). Unloading from point B and reversing the load into compression leads to point A again. One complete traverse along this route is shown in figure 2.2, and forms a hysteresis loop. A complete cycle such as that between points A and B includes two reversals in the direction of loading. It is the best way to describe the material's behavior on the basis of stress and strain during cyclic loading. Apart from showing cyclically varying stresses, the hysteresis loop provides a measure of plastic strains per cycle.

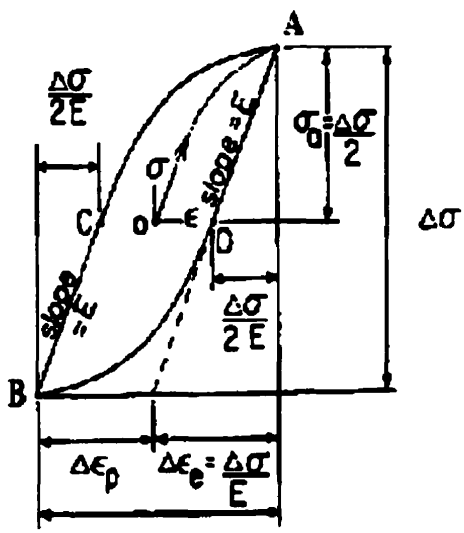

Figure 2.2 Standard Hysteresis loop

2.3 Material Stress-Strain Curve

Behavior of a material in response to an applied loading is represented using a stress-strain curve. Regardless of the method used in engineering design, analysis to determine stresses and strains always requires the use of appropriate stress-strain relationships for the particular material. Various stress-strain relationships have been proposed to characterize the non-linear behavior of materials. The Ramberg-Osgood stress-strain relationship [4] is one such relationship that provides a reasonably accurate representation of the stress-strain curve of real materials. It differs from the other relationships in that there is no distinct yield point. At all values of stress, elastic strain (ε_e) and plastic strain (ε_p) are summed to obtain total strain, resulting in a smooth continuous curve. Elastic strain is linearly related to stress by Young's Modulus, E, whereas the plastic strain is related to stress by an exponential relationship.

The Ramberg-Osgood relationship [4] between stress and total strain is given as:

$$\varepsilon = \varepsilon_e + \varepsilon_p = \frac{\sigma}{E} + \left(\frac{\sigma}{K}\right)^{1/n} \tag{2.1}$$

According to Dowling [5] the stress-strain paths for cyclic loading are predicted to follow a path that is given by a factor-of-two expansion of the monotonic stress-strain curve.

$$\frac{\Delta\varepsilon}{2} = f\left(\frac{\Delta\sigma}{2}\right) = \frac{\Delta\sigma}{2E} + \left(\frac{\Delta\sigma}{2K'}\right)^{1/n'} \tag{2.2}$$

where $\varepsilon = f(\sigma)$ is the monotonic curve.

2.3.1 Plane Stress Condition

For stable cyclic loading following completion of most cycle-dependent hardening or softening, the monotonic curve is replaced with a special cyclic stress-strain curve, with the Ramberg-Osgood form:

$$\varepsilon_a = \frac{\sigma_a}{E} + \left(\frac{\sigma_a}{K'}\right)^{1/n'} \tag{2.3}$$

where σ_a and ε_a are the stress and strain amplitudes and the constants K' and n' correspond to cyclic strength coefficient and cyclic strain hardening exponent, respectively. It should be noted that these material constants differ from those for the monotonic curve.

Equation (2.3) can be further stated as:

$$\varepsilon_a - \frac{\sigma_a}{E} = \left(\frac{\sigma_a}{K'}\right)^{1/n'} \tag{2.4}$$

$$\varepsilon_p = \left(\frac{\sigma_a}{K'}\right)^{1/n'} \tag{2.5}$$

$$\sigma_a = K'\varepsilon_p^{\,n'} \tag{2.6}$$

Taking logarithms on both sides of equation (2.6) gives

$$\log \sigma_a = n' \log \varepsilon_p + \log K' \tag{2.7}$$

On a log-log plot the above equation yields a straight line of the form $y = mx + C$

where

$y = \log \sigma_a$

$x = \log \varepsilon_p$

Slope, m = n'

$$C = \log K'$$

The cyclic stress-strain constants K' and n' are obtained by plotting equation (2.7) and performing a linear regression analysis. K' is the value of the stress at $\varepsilon_p = 1$, and n' is the slope of the line on the log-log plot if the decades of both logarithmic scales have the same length.

2.3.2 Plane Strain Condition

The existence of plane stress or plane strain conditions depends on the thickness of the specimen and the notch-tip radius.

In the plane stress condition, the specimen is thin and there is a uniaxial stress state at the notch-tip. The cyclic material properties obtained from the plain specimen subjected to uniaxial loading can be used to determine the stress-strain relationship under plane stress conditions.

In the case of plane strain condition, the specimen is thicker and there is a biaxial stress state at the notch-tip. The plain specimen cyclic stress-strain curve is no longer valid. Uniaxial stress-strain curve can be translated into an analogous plane strain relation using the following expressions developed by Dowling [6]:

$$\sigma^* = \frac{\sigma}{\sqrt{(1-\mu+\mu^2)}} \tag{2.8}$$

$$\varepsilon^* = \frac{\varepsilon(1-\mu^2)}{\sqrt{(1-\mu+\mu^2)}} \tag{2.9}$$

where $\mu = \dfrac{\upsilon + E\varepsilon_p/2\sigma}{1 + E\varepsilon_p/\sigma}$; $\varepsilon_p = \varepsilon - \dfrac{\sigma}{E}$; υ : Poisson's ratio

Using these relations the stress-strain curve under biaxial 'plane strain' conditions using plane strain values can be deduced as,

$$\varepsilon^* = \frac{\sigma^*}{E}(1-\upsilon^2) + \left(\frac{\sigma^*}{K^*}\right)^{1/n^*} \tag{2.10}$$

In the case of cyclic loading,

$$\frac{\Delta\varepsilon^*}{2} = \frac{\Delta\sigma^*}{2E}(1-\upsilon^2) + \left(\frac{\Delta\sigma^*}{2K^*}\right)^{1/n^*} \tag{2.11}$$

In terms of stress and strain amplitudes,

$$\varepsilon_a^* = \frac{\sigma_a^*}{E}(1-\upsilon^2) + \left(\frac{\sigma_a^*}{K^*}\right)^{1/n^*} \tag{2.12}$$

2.4 Literature Search

The design of mechanical components to counter fatigue is associated with the estimation of stress-strains at the fatigue critical locations. A number of books and articles suggest that between 50 and 90 percent of all the mechanical failures are due to fatigue; most of these are unexpected fractures.

August Wöhler [7], in the 1850s, motivated by the frequently occurring failures under repeated loading, started off with extensive experimentation. These experiments were

concerned with railway axle failures and were considered to be the first systematic investigation of fatigue. He showed from stress vs. life (S-N) diagrams how fatigue life decreased with higher stress amplitudes and that below a certain stress amplitude, the test specimen did not fracture. It was Wöhler who introduced the concept of the S-N diagram and the fatigue limit.

During the 1870s and 1890s other researchers substantiated and expanded Wöhler's classical work. Among them were Gerber and Goodman, who made exceptional contributions to this study by introducing the influence of mean stresses on fatigue life. The early work on fatigue and subsequent efforts to the 1950s were reviewed in a paper by Mann [8].

In the early 1960s low cycle strain-controlled fatigue behavior became prominent following the development of the Coffin-Manson [1], [2] relationship between plastic strain amplitude and fatigue life. Extensive research was carried out by various researchers, particularly the works contributed by JoDean Morrow [9], [10], Bela I. Sandor [11], [12], Darrel Socie [13], led to clear concepts of fatigue damage. It was concluded that the cause of fatigue damage was *cyclic plasticity* [12]. There is enough information available at present to help one appreciate the role of plastic strains in fatigue. Yet the current technology, particularly *instrumentation* is not adequate for the accurate measurement of cyclic plastic strains in a sufficient variety of situations.

In 1961, Neuber published his theory of stress concentration [14], where he proposed a relationship (later known as Neuber's rule), between nominal and notch-tip stress and strain in terms of elastic stress and strain concentration factors. Neuber's rule complimented the Manson-Coffin relationship in estimating fatigue life. However, the studies to verify Neuber's rule by Lieis *et al.* [15] and Conle *et al.* [16] revealed that it *may* overestimate the local inelastic strains and stresses. More recently, Seeger and Heuler [17] derived a more general form of Neuber's rule.

Hutchinson [18], for cracks, and Walker [19], for deep sharp notches, found that in the case of localized plastic yielding the energy density distribution in the plastic zone is almost the same as in the linear elastic material. Molski and Glinka [20], proposed the Equivalent Strain-Energy Density (ESED) method based on the energy density criteria developed by Hutchinson and Walker, to estimate notch-tip inelastic stress-strains. The energy approach was found to be superior to Neuber's rule [20]. When compared with the experimental notch-tip strains, it was found to slightly underestimate the experimental data. Glinka [21] modified the ESED method by introducing a plastic zone size correction parameter, thereby eliminating the underestimation. Further it was successfully used to estimate the fatigue life in low cycle and high cycle fatigue range.

In late 1980s, an improved Neuber's rule was proposed by Wu [22], based on the hypothesis that the Neuber's rule is approximate in nature and its accuracy depended on the specific material properties. Results based on the improved Neuber's rule were quite

encouraging in both plane stress as well as plane strain conditions. When applied to low cycle fatigue (LCF) life estimation, it was found that the results were far better than those estimates obtained using Neuber's rule. A comprehensive source of information and references on local strain approach and fatigue life predictions in a notched member, are available in reference [6].

2.5 SAE Compact Tension Keyhole Specimen Description and Loading

The specimen used for purposes of this work was originally designed by the SAE Fatigue Design and Evaluation Committee [6] &[23]. Every possible effort has been made by the SAE committee, to incorporate similar conditions on the notch-tip of the specimen as experienced by the components in service.

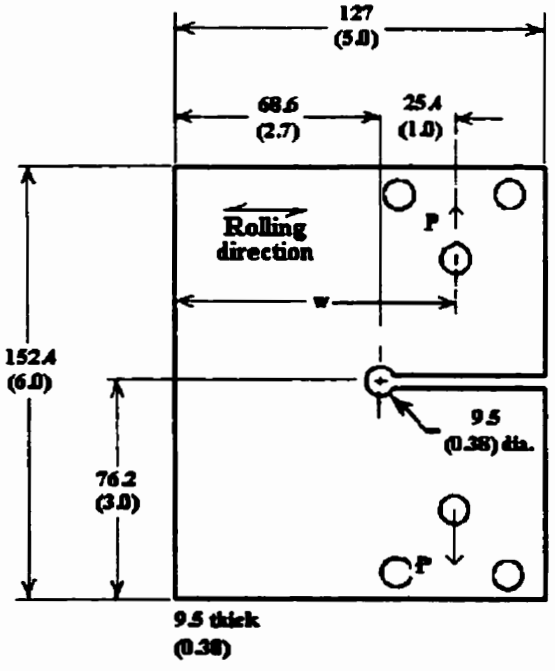

Figure 2.3 SAE Keyhole CCT Specimen [23]
[All dimensions are in mm (inch)]

For each alloy, specimens were cut from a single heat of 3/8" hot rolled plate. The rolling direction used by the SAE was perpendicular to the applied load. A hole was drilled and then saw cut from one side to provide the notch. Reaming with no edge preparation which left the specimen with a notch condition similar to that of many production parts.

The SAE committee in their test program [23] applied loading through a close tolerance monoball fixture which allowed both tensile and compressive loading. Similar loading conditions are assumed in the present evaluation where a nominal stress amplitude S_a(MPa) is applied to the specimen. As the notch-tip in the SAE keyhole specimen is under the combined effect of bending and tension, the nominal stress in the notch-tip is calculated from:

$$S_a = \frac{Mz}{I} + \frac{P}{A} \tag{2.13}$$

$$\text{or } S_a = 11.265\ P$$

for P in (KN) and S_a (MPa). The above derivation is based on the assumption that the net section of the keyhole specimen is subjected to both bending and axial loading. Moment M, is calculated about the neutral axis of the net section. Derivation of equation (2.13) is presented in Appendix C.

Chapter Three

LOCAL STRESS-STRAIN METHODS

3.1 Introduction

Almost all machine components and structural members contain some form of geometrical or microstructural discontinuities. These discontinuities, which are unavoidable in design, include holes, fillets, grooves, keyways, and cause the applied stress to be locally elevated. They are called stress raisers. Stress raisers, generically termed 'notches' for brevity, require special attention as their presence reduces the resistance of a component to fatigue failure.

The magnitude of notch-tip strain depends on the applied stress and the notch geometry. It is usually of high magnitude and plastically deforms the material in the vicinity of the notch. Notch-tip strain is the basic controlling parameter which alters the microstructure and causes grain slip in materials, leading to the initiation of fatigue crack. Further, as noted previously, it has been proposed [23] that a notched specimen's fatigue initiation life can be estimated by comparison with that of a plain specimen subjected to the same strain history as the notch-tip. This requires either measurement or calculation of local notch-tip

strains. Often the measurement and control of cyclic strains in the neighborhood of complex notch geometries either requires extremely sophisticated instrumentation or is almost impossible to accomplish. Although the finite element method and the boundary integral method represent tools which enable accurate calculations for static loading, less complex approaches are obviously preferable and they are often the only practical methods for lengthy cyclic loading histories. Therefore, it can be emphasized that there is a desperate need for a simpler analytical approach to calculate cyclic notch-tip strains.

So far the local stress-strain methods are considered the simplest. In this present work, three local stress-strain methods which are frequently used in today's industry are considered for evaluation. They are:

1. Neuber's rule
2. Improved Neuber's rule and
3. Equivalent Strain-Energy Density (ESED) Method.

3.2 Neuber's Rule

The theoretical stress concentration factor, K_t, is often used to relate the nominal stresses, S_a, or strains e, to the local values at notch tip, σ and ε. For increasing nominal stress S_a, K_t remains constant until yielding begins. Upon yielding, the local stress, σ, and local strain ε, are no longer linearly related and the local values are no longer related to the nominal values by K_t. Instead, the nominal and local values are related in terms of stress and strain concentration factors.

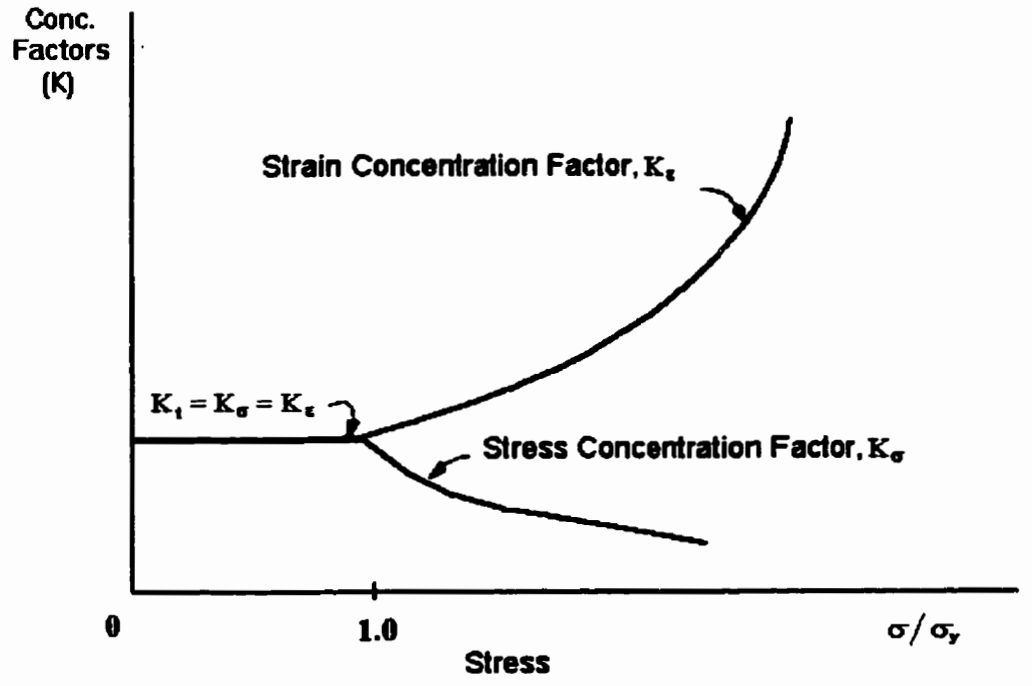

Figure 3.1 Effect of yielding on K_σ and K_ε

Neuber's rule [14] states that the theoretical stress concentration is the geometric mean of the stress and strain concentration factors.

$$K_t = \sqrt{K_\sigma K_\varepsilon} \tag{3.1}$$

where $K_\sigma = \frac{\sigma}{S_t}$ and $K_\varepsilon = \frac{\varepsilon}{e}$ for $\sigma > \sigma_y$

This seems intuitively reasonable since after yielding occurs, K_σ decreases while K_ε increases as shown in the figure 3.1.

Notch response in terms of the applied load under plane stress conditions can be expressed as,

$$\sigma \varepsilon = \frac{(K_t S_t)^2}{E} \tag{3.2}$$

For a cyclic applied load range ΔS,

$$\Delta\sigma\Delta\varepsilon = \frac{(K_t \Delta S)^2}{E} \tag{3.3}$$

The above relation can be further written in terms of amplitudes, since $\Delta S = 2S_a$, $\Delta\sigma = 2\sigma_a$ and $\Delta\varepsilon = 2\varepsilon_a$,

$$\sigma_a \varepsilon_a = \frac{(K_t S_a)^2}{E} \tag{3.4}$$

Local stress-strains amplitudes are to be determined while the values on the right hand side, which are basically constants for an applied load, are usually known.

Thus,

$$\sigma_a \varepsilon_a = \text{constant} \tag{3.5}$$

Mathematically, the above equation is a hyperbola.

The cyclic stress-strain curve of the material in terms of local stress-strain amplitudes under plane stress is given as:

$$\varepsilon_a = \frac{\sigma_a}{E} + \left(\frac{\sigma_a}{K'}\right)^{1/n'} \tag{3.6}$$

Since the notch stress-strain response must lie on the cyclic stress-strain curve of the material, the intersection of the above two curves (equations 3.4 and 3.6) provides the values of σ_a and ε_a for the nominal loading S_a. This can be obtained by solving the two non-linear equations for σ_a and ε_a using numerical methods.

$$\left(\frac{\sigma_a}{E}+\left(\frac{\sigma_a}{K'}\right)^{1/n'}\right)\sigma_a=\frac{(K_t S_a)^2}{E} \tag{3.7}$$

Topper *et al.*[10] have extended Neuber's rule to fatigue problems by replacing K_t with K_f.

$$\left(\frac{\sigma_a}{E}+\left(\frac{\sigma_a}{K'}\right)^{1/n'}\right)\sigma_a=\frac{(K_f S_a)^2}{E} \tag{3.8}$$

where $K_f=1+\left(\frac{K_t-1}{1+\frac{a}{\rho}}\right)$

Although, such a substitution made it possible to improve the fatigue life prediction at times, it did not improve the accuracy of the calculated notch strains. For this reason, K_t was used instead of fatigue notch factor, K_f for evaluating the local stress-strain methods.

In the present work, a frequently used iterative technique -- the bisection method -- is used for solving equation (3.7) for σ_a. Further, the local strain amplitude ε_a, can be obtained by substituting σ_a in the Ramberg-Osgood relation (equation 3.6).

Notch-tip response under plane strain conditions can be expressed as,

$$\sigma^*{}_a\varepsilon^*{}_a=\frac{(K_t S_a)^2}{E^*} \tag{3.9}$$

where $E^*=\frac{E}{(1-\upsilon^2)}$.

Equations (2.12) and (3.9) can be solved for notch-tip stress-strains under plane strain conditions.

3.3 Improved Neuber's Rule

Neuber's rule is widely used for local stress-strain analysis and for low cycle fatigue life estimation. However, it was found by Mowbray and McConnolee [24] that Neuber's rule often overestimates the notch-tip strains and stresses. The accuracy of the Neuber-based strain calculations can vary [16], [25] depending on several factors including the material stress-strain curve, the stress-concentration factor and the nominal stress level. Efforts were being made to improve the conventional Neuber's rule. Recently one such improvement was proposed by Wu [22], which was based on the hypothesis that the accuracy of Neuber's rule is dependent on the material properties. Finite element analysis [22] was carried out using an SAE keyhole compact tension specimen [CCT specimen]. Twenty different material properties were studied in plane stress and plane strain conditions. A new parameter m , pertaining to the material properties, was introduced in Neuber's rule. The study of the relationship between m (exponent) and the material properties revealed that the parameter m increased with increasing n' and decreased with increasing K'/E.

For a CCT specimen, the parameter m was found to be related to the material properties as

$m = 0.48 + 0.31\ n' - 8.60\ K'/E$ in the plane stress condition. (3.10)

$m = 0.42 + 0.25\ n^* - 3.92\ K^*/E^*$ in the plane strain condition. (3.11)

The least squares method was used to determine the value of m.

The improved Neuber's rule [22] exhibits the format :

$$K_t = K_\sigma^{\ m} K_\varepsilon^{(1-m)} \tag{3.12}$$

For cyclic loading,

$$K_t \Delta S = (\Delta\sigma)^m (E\Delta\varepsilon)^{1-m} \tag{3.13}$$

In terms of stress-strain amplitudes, the above equation can be rewritten as

$$K_t S_a = (\sigma_a)^m (E\varepsilon_a)^{1-m} \tag{3.14}$$

Substituting ε_a from equation (3.6) in (3.14), results in a non-linear equation in σ_a.

$$\varepsilon_a = \frac{\sigma_a}{E} + \left(\frac{\sigma_a}{K'}\right)^{1/n'} = \left(\frac{K_t S_a}{E^{1-m}\sigma_a{}^m}\right)^{1/1-m} \tag{3.15}$$

The above equation is solved for stress amplitude, using standard iterative techniques. The bisection method is used here. Strain amplitude ε_a under plane stress, can then be calculated by substituting σ_a back into the material stress-strain relation.

Notch response in plane strain can be expressed as,

$$K_t S_a = (\sigma^*{}_a)^m (E^* \varepsilon^*{}_a)^{1-m} \tag{3.16}$$

Similarly, under plane strain conditions, equation (3.16) is solved along with the stress-strain curve of the plane strain condition [equation (2.12)] to obtain notch-tip stress-strains under applied cyclic loading.

3.4 Equivalent Strain-Energy Density (ESED) Method

It has been shown by Hutchinson [18], for cracks, and by Walker [19], for deep sharp notches, that in the case of localized plastic yielding, the energy density distribution in the plastic zone is almost the same as in linear elastic material. This implies, in the presence of

localized small scale plastic yielding, the gross linear elastic behavior of the material surrounding the notch controls the deformations in the plastic zone. Therefore, the strain-energy density in the crack-tip plastic zone can be calculated on the basis of the elastic stress field as derived by means of the theory of elasticity. However, due to the stress redistribution caused by the plastic flow (*i.e.*, due to local unloading), the plastic zone and the strain-energy density increase slightly in comparison to the purely linear elastic estimations. A plastic zone correction factor C_p, has been introduced by Glinka [21], to take care of such an increase in the plastic zone size. The derivation of C_p is based on Irwin's plastic-zone correction [26] analogy, where it is assumed that an increase in the hypothetical elastic stress σ_e , [as shown in figure 3.2] near the notch-tip leads to an increase of the strain-energy density in the plastic zone W_p.

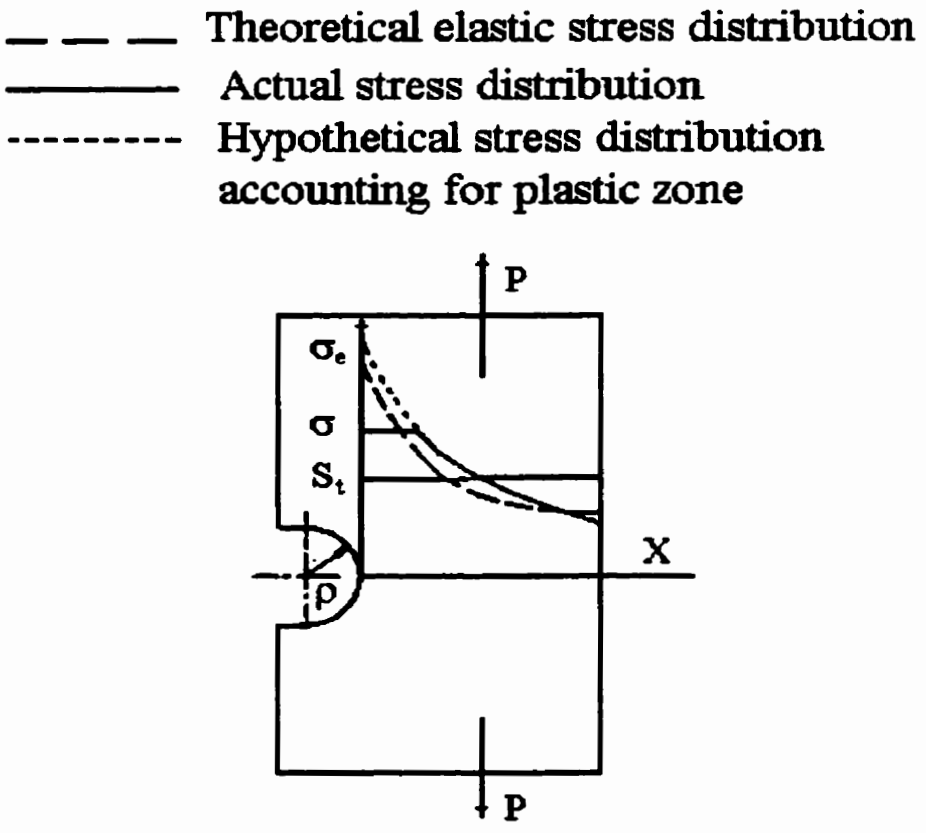

Figure 3.2 Elastic stress distribution near a notch-tip

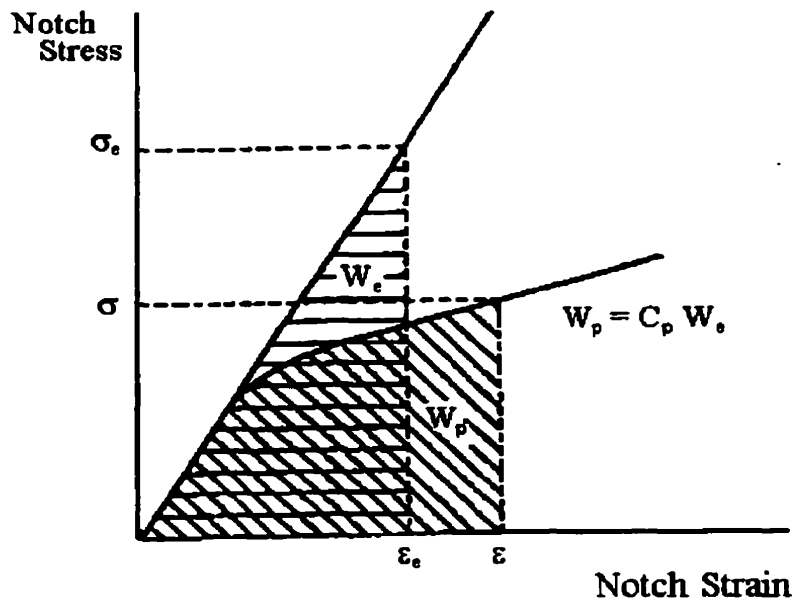

Figure 3.3 Graphical Representation of ESED concept

Details on the ESED method and the derivation of C_p are elaborately presented in references [21] & [27].

The strain-energy density in the plastic zone can be written as

$$W_p = C_p W_e \tag{3.17}$$

The graphical interpretation of the equivalent strain-energy density hypothesis is shown in figure 3.3. The hatched triangular area under the linear material stress-strain represents the strain-energy W_e due to the hypothetical elastic stress.

Strain-energy density W_p in the notch-tip can be written in the form [27], [28]

$$W_p = \frac{C_p (K_t S_t)^2}{2E} \qquad \text{for plane stress condition} \qquad (3.18)$$

and $$W_p = \frac{C_p^{\bullet} (K_t S_t)^2}{2E}(1-\upsilon^2) \qquad \text{for plane strain condition} \qquad (3.19)$$

where $$C_p = \frac{2 - \frac{1}{2}\left(\frac{\rho}{r_p}\right) + \frac{1}{4}\left(\frac{\rho}{r_p}\right)^2}{1 + \frac{1}{2}\left(\frac{\rho}{r_p}\right)} \text{ and } C_p^{\bullet} = \frac{2 - \frac{1}{2}\left(\frac{\rho}{r_p^{\bullet}}\right) + \frac{1}{4}\left(\frac{\rho}{r_p^{\bullet}}\right)^2}{1 + \frac{1}{2}\left(\frac{\rho}{r_p^{\bullet}}\right)}$$

It should be noted that the plastic zone correction factor, C_p can be neglected [27] for blunt notches of $K_t < 2.5$ in the strain hardening materials where the nominal stress in the notch-tip is less than 80 percent of the yield stress. Further, C_p is a function of notch tip radius ρ and the plastic zone size r_p.

3.4.1 Estimation of Plastic zone size r_p

Under the assumption of localized plasticity, the first approximation of the plastic zone size r_p ahead of the notch-tip can be derived from the Hencky-Mises-Huber criterion [27]. In plane stress condition,

$$\sigma_{ys} = \frac{K_t S_a}{2\sqrt{2}} \left[\frac{\rho}{r_p} + \frac{3}{4}\left(\frac{\rho}{r_p}\right)^3 \right]^{1/2} \qquad (3.20)$$

and in plane strain condition,

$$\sigma_{ys}^{\bullet} = \frac{K_t S_a}{2\sqrt{2}} \left[\frac{\rho}{r_p^{\bullet}}(1-2\upsilon)^2 + \frac{3}{4}\left(\frac{\rho}{r_p^{\bullet}}\right)^3 \right]^{1/2} \qquad (3.21)$$

Equations (3.20), (3.21) can be solved for the plastic zone size, using bisection method. This technique is included in the computer code listed in appendix A. A detailed derivation of the above equations is presented in references [27] and [28]. It should be noted that C_p^* relies on r_p^* which in turn depends on the material yield strength under plane strain conditions σ_{ys}^*.

3.4.2 ESED Under Plane Stress

The strain-energy density W_p in the notch-tip can also be related to the local stresses and elasto-plastic strains in the notch-tip. Using the Ramberg Osgood stress-strain equation, the relationship after the integration can be expressed as [21],

$$W_p = \frac{\sigma^2}{2E} + \frac{\sigma}{n'+1}\left(\frac{\sigma}{K'}\right)^{1/n'} \tag{3.22}$$

By equating equations (3.18) and (3.22), the following expression for plane stress relating the nominal elastic stress, S_a in the net cross section and the actual notch-tip stress in the plastically deformed notch-tip can be derived.

$$\frac{C_p(K_t S_t)^2}{2E} = \frac{\sigma^2}{2E} + \frac{\sigma}{n'+1}\left(\frac{\sigma}{K'}\right)^{1/n'} \tag{3.23}$$

In the case of cyclic loading, the nominal stress and the notch-tip stress have to be replaced by stress ranges. Therefore, for plane stress :

$$\frac{C_p(K_t \Delta S_t)^2}{2E} = \frac{\Delta\sigma^2}{2E} + \frac{\Delta\sigma}{n'+1}\left(\frac{\Delta\sigma}{K'}\right)^{1/n'} \tag{3.24}$$

In terms of stress-strain amplitudes,

N, the total strain is the sum of the sum of the elastic and plastic strains. At large strains or short lives (low cycle fatigue), the plastic strain component is predominant, and at small strains or longer lives (high cycle fatigue) the elastic strain component is predominant. There are three standard approaches used in the industry towards fatigue analysis. Namely,

1. Stress life approach
2. Strain life approach and
3. Fracture mechanics approach.

Each of these have certain strengths and weaknesses depending on the area of application. The strain life approach is found to give a reasonably fair estimate of crack initiation life whereas the fracture mechanics approach is good at crack propagation life. A combination of these two approaches can provide an excellent total fatigue life estimate [29].

In a notched component or specimen subjected to external cyclic loads, the behavior of material at the root of the notch is best considered in terms of strain. As long as there is an elastic constraint surrounding the local plastic zone at the notch, the strain can be calculated more easily than the stress [30]. The present work is focused on the automotive industry, where crack initiation is usually regarded as the failure criteria. Therefore a strain-based approach has been adopted to estimate fatigue crack initiation life for the SAE compact tension keyhole specimen.

Strain life curves are usually plotted on a log-log scale with number of reversals to failure (2N) as the abscissa and the total strain amplitude as the ordinate. The total strain amplitude can be resolved into the elastic and plastic strain components from the steady-state hyteresis loop. At a given life (2N), the total strain is the sum of the elastic and plastic strain components.

The strain-life data for smooth axial specimens is given by :

$$\frac{\Delta\varepsilon}{2} = \frac{\Delta\varepsilon_e}{2} + \frac{\Delta\varepsilon_p}{2} \tag{3.28}$$

In terms of strain amplitude,

$$\varepsilon_a = \varepsilon_e + \varepsilon_p \tag{3.29}$$

Therefore,

$$\varepsilon_a = \frac{\sigma_f'}{E}(2N)^b + \varepsilon_f'(2N)^c \tag{3.30}$$

The above relation is known as Coffin-Manson relationship [1], [2] -- which is quite popular and the most frequently used relation in fatigue life estimation in today's industry. Interested reader can refer to any introductory book on metal fatigue, such as references [29] or [30] for a detailed description on Coffin-Manson relationship and strain-life curve.

The quantities σ_f', b, ε_f', and c are considered to be material properties and are usually referred to as the strain-life constants or fatigue properties. Strain-life data in the form of simplified fatigue material properties have been accumulated and published in reference [31].

The inclusion of mean stress or mean strain effects in fatigue life prediction methods involving strain-life data is found to be very complex. One method is to replace σ_f' with $(\sigma_f'-\sigma_m)$ in the Coffin-Manson relation, where σ_m is the mean stress, such that

$$\varepsilon_a = \frac{\sigma_f' - \sigma_m}{E}(2N)^b + \varepsilon_f'(2N)^c \tag{3.31}$$

σ_m is taken as positive for tensile values and negative for compressive values. The above equation is frequently referred to as the modified version of the Morrow approach [32].

3.6 Effect of Residual Stress

Almost all manufactured parts carry stresses that are in equilibrium within the part, without an externally applied load. These are called the self-stresses or residual stresses.

Mechanical or thermal processes such as shot-peening, surface rolling, welding, drilling, and surface hardening produce residual stresses in the manufactured components. They can improve or ruin the life in the components which are subjected to cyclic loading for all long-life (high cycle) and intermediate-life fatigue applications. Compressive mean stresses are found to have a beneficial effect on the fatigue life of the components whereas tensile stresses are the root cause for fatigue failures.

As the present work is more focused on the low cycle fatigue range where residual stresses have little effect on fatigue life, the residual stresses will not be considered.

Chapter Four

RESULTS AND DISCUSSION

The results obtained from the different local stress-strain methods will be presented in this chapter. The notch-tip strains and fatigue crack initiation life estimates obtained from the three local stress-strain methods will be compared with published experimental results in plane stress and plane strain conditions. This will be followed by a discussion on significant observations, leading to some meaningful conclusions.

The experimental notch-tip strains and fatigue crack initiation life estimates for a keyhole SAE compact tension specimen made of two commercial automotive steels as reported in [6], are used in the present study. Further, it has been reported in [23] that the finite element notch-tip calculations for the SAE keyhole specimen were found to agree very closely with the measured strains at the notch-tip.

4.1 Material Stress-strain curves

Figures 4.1 and 4.2 show the uniaxial σ - ε curve and the biaxial plane strain curve σ_i - ε_i data for RQC-100 and MAN-TEN steel and their cyclic material and fatigue properties are tabulated in tables 4.1 to 4.3.

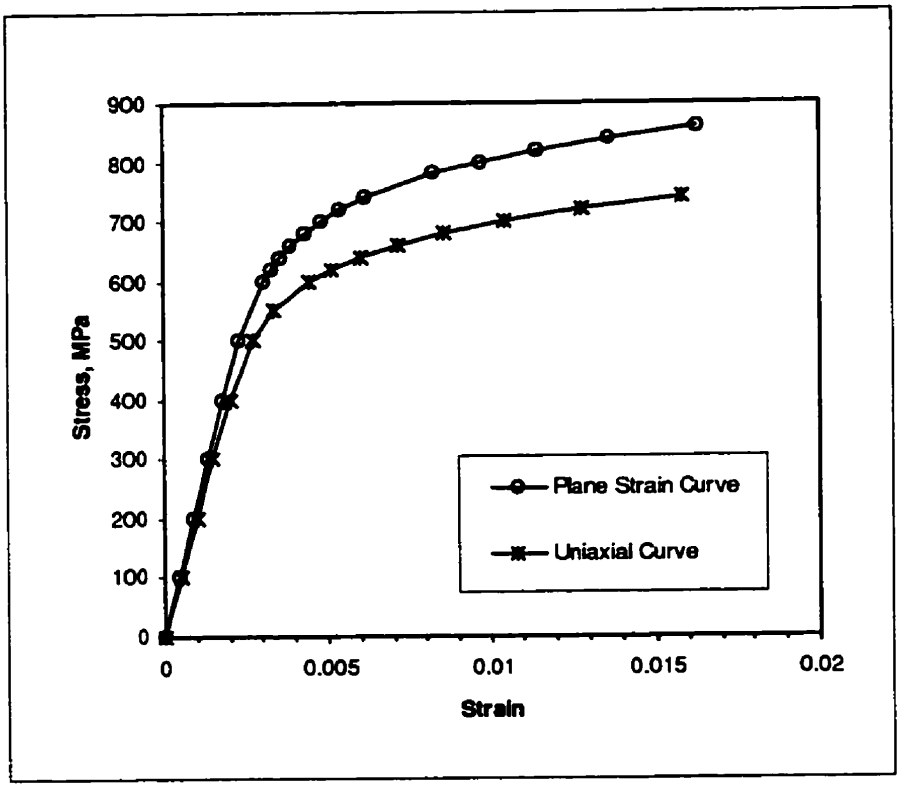

Figure 4.1 : Uniaxial σ - ε curve and the Biaxial plane strain σ_i - ε_i curve for RQC-100 Steel

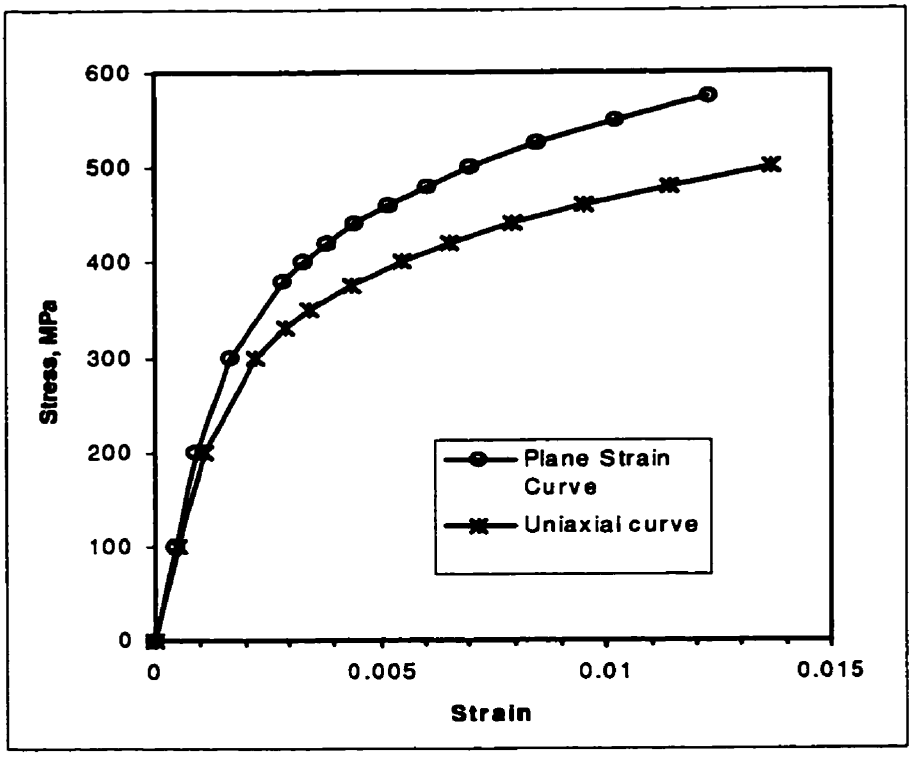

Figure 4.2 : Uniaxial σ - ε curve and the Biaxial plane strain σ_i - ε_i curve for MAN-TEN Steel

A biaxial stress state exists at the notch-tip under plane strain conditions. Therefore the cyclic properties obtained from plain specimens subjected to uniaxial loading are no longer applicable. However, cyclic properties in plane strain can be derived by the transformation of the uniaxial σ - ε curve using the expressions suggested by Dowling [6].

The cyclic strength coefficient, K^* and the cyclic strain hardening exponent, n^* in plane strain conditions are obtained using a linear regression analysis analogous to the method recommended by ASTM [33] for the determination of parameters K' and n' for the uniaxial stress-strain relationship.

The cyclic material properties K^* and n^* along with the yield strength σ^*_{ys} for both the materials were found to be larger than their corresponding values in the uniaxial case.

4.2 Evaluation of methods under plane stress and plane strain conditions

The calculated and experimental notch-tip strains under simple harmonic loading for both materials under plane stress and plane strain conditions are listed in tables 4.5 to 4.10 and are presented in figures 4.3 to 4.6.

It is evident that Neuber's rule overestimated the notch-tip strains in plane stress as well as in plane strain conditions, which substantiates the results reported by various researchers [15], [16], [20].

Material Property	Plane Stress	Plane Strain
Young's modulus (E, E^*), MPa	203000	223077
Yield strength (σ_{ys}, σ^*_{ys}), MPa	620	720
Strength coefficient (K', K^*), MPa	1150	1344
Strain hardening exponent (n', n^*)	0.1	0.1017

Table 4.1 Smooth specimen stress-strain properties for RQC-100 [23]

Material Property	Plane Stress	Plane Strain
Young's modulus (E, E^*), MPa	203000	223077
Yield strength (σ_{ys}, σ^*_{ys}), MPa	330	420
Strength coefficient (K', K^*), MPa	1190	1427
Strain hardening exponent (n', n^*)	0.193	0.1962

Table 4.2 Smooth specimen stress-strain properties for MAN-TEN [23]

Property	RQC-100	MAN-TEN
Fatigue strength coefficient, σ'_f, MPa	1165	930
Fatigue strength exponent, b	-0.075	-0.095
Fatigue ductility coefficient, ε'_f	1.06	0.26
Fatigue ductility exponent, c	-0.75	-0.47

Table 4.3 Fatigue properties for RQC-100 and MAN-TEN steels [23]

Parameter	Value
Elastic Stress Conc. Factor, K_t	3.0
Peterson's parameter, a	0.0025 in.
Notch-tip radius, ρ	0.187 in.

Table 4.4 Notch-tip parameters for SAE keyhole specimen [23]

Notch-tip Strains, ε_a					Reversals to Failure, 2N		
P (KN)	Sa (MPa)	Neuber	Improved Neuber	ESED	Neuber	Improved Neuber	ESED
13.32	150	0.00225	0.00225	0.00222	390570	401396	448939
17.75	200	0.00325	0.00323	0.00302	23560	24568	36050
22.19	250	0.00459	0.00447	0.00394	5823	6342	9943
26.63	300	0.00620	0.00596	0.00507	2487	2756	4273
31.07	350	0.00809	0.00763	0.00643	1354	1535	2277
35.51	400	0.01029	0.00950	0.00803	835	974	1374
39.95	450	0.01293	0.01156	0.00990	549	671	900
44.38	500	0.01637	0.01377	0.01203	365	491	624
48.82	550	0.02149	0.01617	0.01444	235	373	452
53.26	600	0.03008	0.01870	0.01713	139	293	339
57.70	650	0.04566	0.02140	0.02010	75	236	261
62.14	700	0.07453	0.02425	0.02335	37	194	206

Table : 4.5 Results under Plane Stress -- RQC-100 Steel

Notch-tip Strains, ε_a					Reversals to Failure, 2N		
P (KN)	Sa (MPa)	Neuber	Improved Neuber	ESED	Neuber	Improved Neuber	ESED
11.54	130	0.00246	0.00242	0.00213	144361	154643	269528
12.43	140	0.00275	0.00268	0.00234	92451	102279	176927
15.09	170	0.00375	0.00357	0.00308	30294	35780	60859
21.31	240	0.00720	0.00606	0.00531	4240	6882	10150
22.19	250	0.00789	0.00647	0.00569	3307	5722	8270
24.86	280	0.01038	0.00774	0.00693	1600	3475	4714
30.18	340	0.01830	0.01053	0.00984	392	1542	1839
31.07	350	0.02016	0.01104	0.01038	311	1367	1602
34.62	390	0.02971	0.01313	0.01269	126	883	962

Table : 4.6 Results under Plane Stress -- MAN-TEN Steel

Notch-tip Strains, ε_n					Reversals to Failure, 2N		
P (KN)	Sa (MPa)	Neuber	Improved Neuber	ESED	Neuber	Improved Neuber	ESED
13.32	150	0.00203	0.00202	0.00202	452231	463510	472105
17.75	200	0.00281	0.00278	0.00271	34106	35966	41883
22.19	250	0.00384	0.00373	0.00347	8592	9520	12556
26.63	300	0.00511	0.00483	0.00431	3598	4180	5827
31.07	350	0.00660	0.00609	0.00530	1932	2320	3270
35.51	400	0.00830	0.00745	0.00643	1190	1486	2051
39.95	450	0.01024	0.00894	0.00770	796	1028	1386
44.38	500	0.01248	0.01054	0.00913	558	754	987
48.82	550	0.01521	0.01224	0.01072	399	578	731
53.26	600	0.01881	0.01404	0.01247	282	456	559
57.70	650	0.02402	0.01592	0.01437	193	370	438
62.14	700	0.03224	0.01790	0.01644	-	306	351

Table : 4.7 Results under Plane Strain -- RQC-100 Steel

Notch-tip Strains, ε_n					Reversals to Failure, 2N		
P (KN)	Sa (MPa)	Neuber	Improved Neuber	ESED	Neuber	Improved Neuber	ESED
11.54	130	0.00207	0.00202	0.00186	230542	260219	368943
12.43	140	0.00230	0.00222	0.00203	150174	174217	251793
15.09	170	0.00307	0.00289	0.00258	51506	64147	97504
21.31	240	0.00549	0.00471	0.00426	8376	13083	19564
22.19	250	0.00593	0.00500	0.00439	6729	10968	16250
24.86	280	0.00746	0.00591	0.00521	3595	6812	9747
30.18	340	0.01179	0.00789	0.00709	1106	3099	4117
31.07	350	0.01274	0.00824	0.00744	913	2761	3625
34.62	390	0.01743	0.00969	0.0089	427	1815	2260

Table : 4.8 Results under Plane Strain -- MAN-TEN Steel

Measured Notch-tip Strains [6]

P (kN)	S_a (MPa)	ε_a
23.08	260	0.004
31.78	358	0.006
39.06	440	0.008
46.52	524	0.01
51.31	578	0.012
56.28	634	0.014
59.83	674	0.016
67.46	760	0.020

Fatigue Crack Initiation life Data [23]

P (kN)	S_a (MPa)	2N
17.8	200	201,000
35.6	403	7200
53.4	602	1300
62.3	702	580
66.7	755	388
88.9	1006	120

Table 4.9 Experimental Results for RQC-100 steel

Measured Notch-tip Strains [6]

P (kN)	S_a (MPa)	ε_a
12.43	140	0.0026
14.91	168	0.0032
20.95	236	0.0049
25.21	284	0.0065
30.18	340	0.0088
34.44	388	0.0102
37.99	428	0.0112
41.54	468	0.0144

Fatigue Crack Initiation life Data [23]

P (kN)	S_a (MPa)	2N
11.36	128	357,000
22.28	251	14400
31.25	352	3580
62.58	705	144

Table 4.10 Experimental Results for MAN-TEN steel

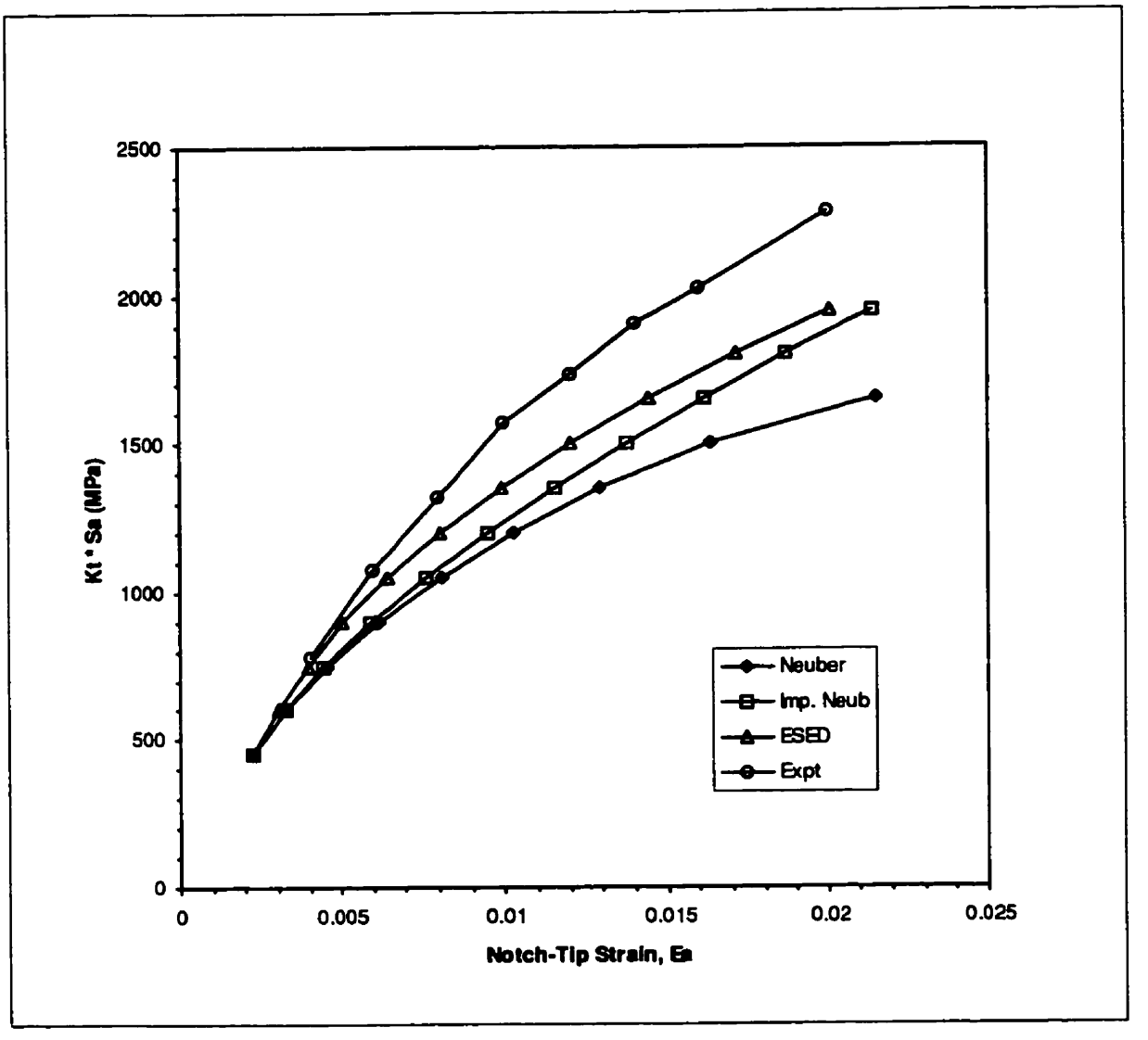

Figure 4.3 : Calculated and experimental Notch-tip strains in a keyhole SAE Compact tension specimen under cyclic loading for RQC-100 steel under *Plane stress* conditions

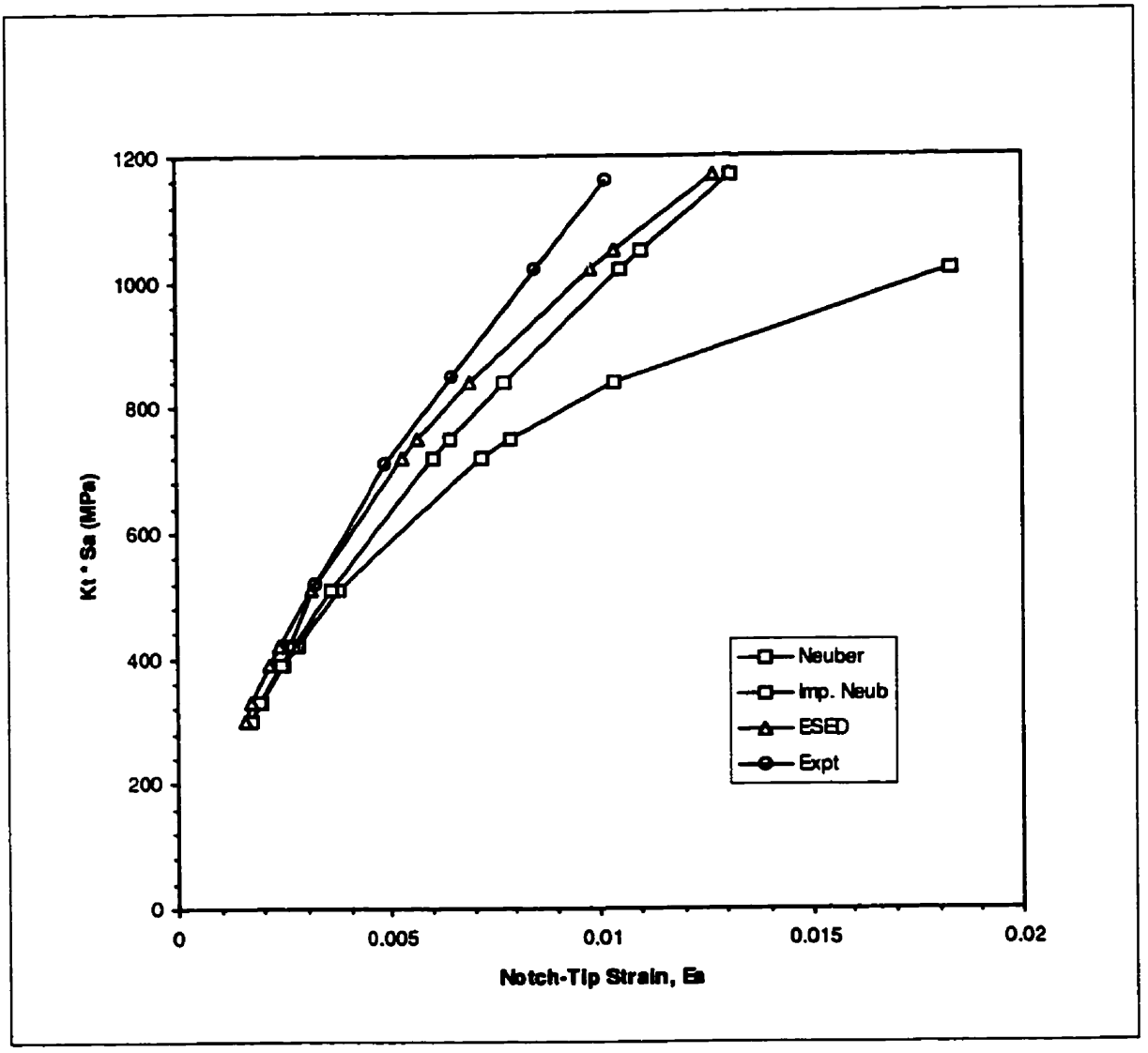

Figure 4.4 : Calculated and experimental Notch-tip strains in a keyhole SAE Compact tension specimen under cyclic loading for MAN-TEN steel under *Plane stress* conditions

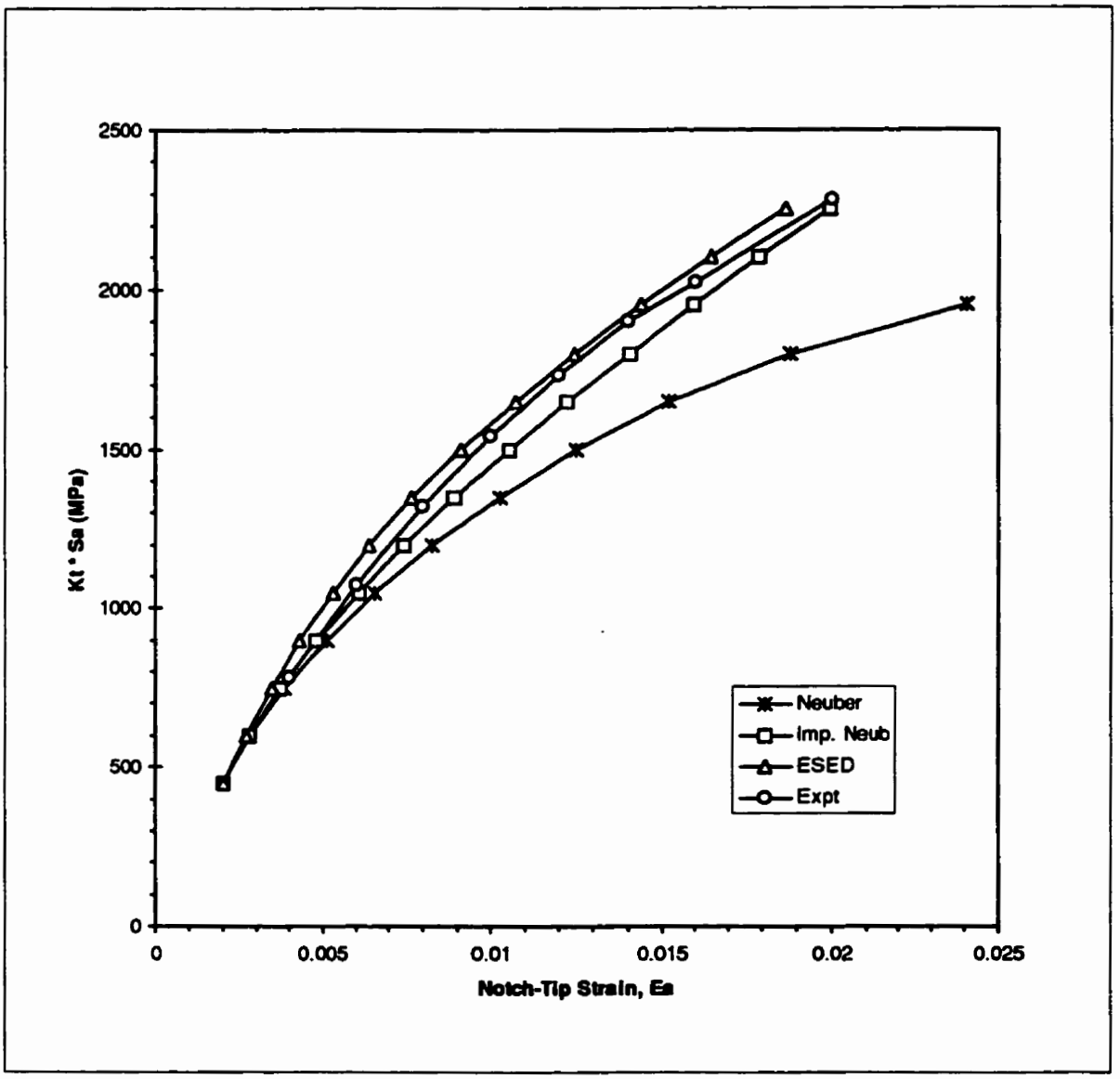

Figure 4.5 : Calculated and experimental Notch-tip strains in a keyhole SAE Compact tension specimen under cyclic loading for RQC-100 steel under *Plane strain* conditions

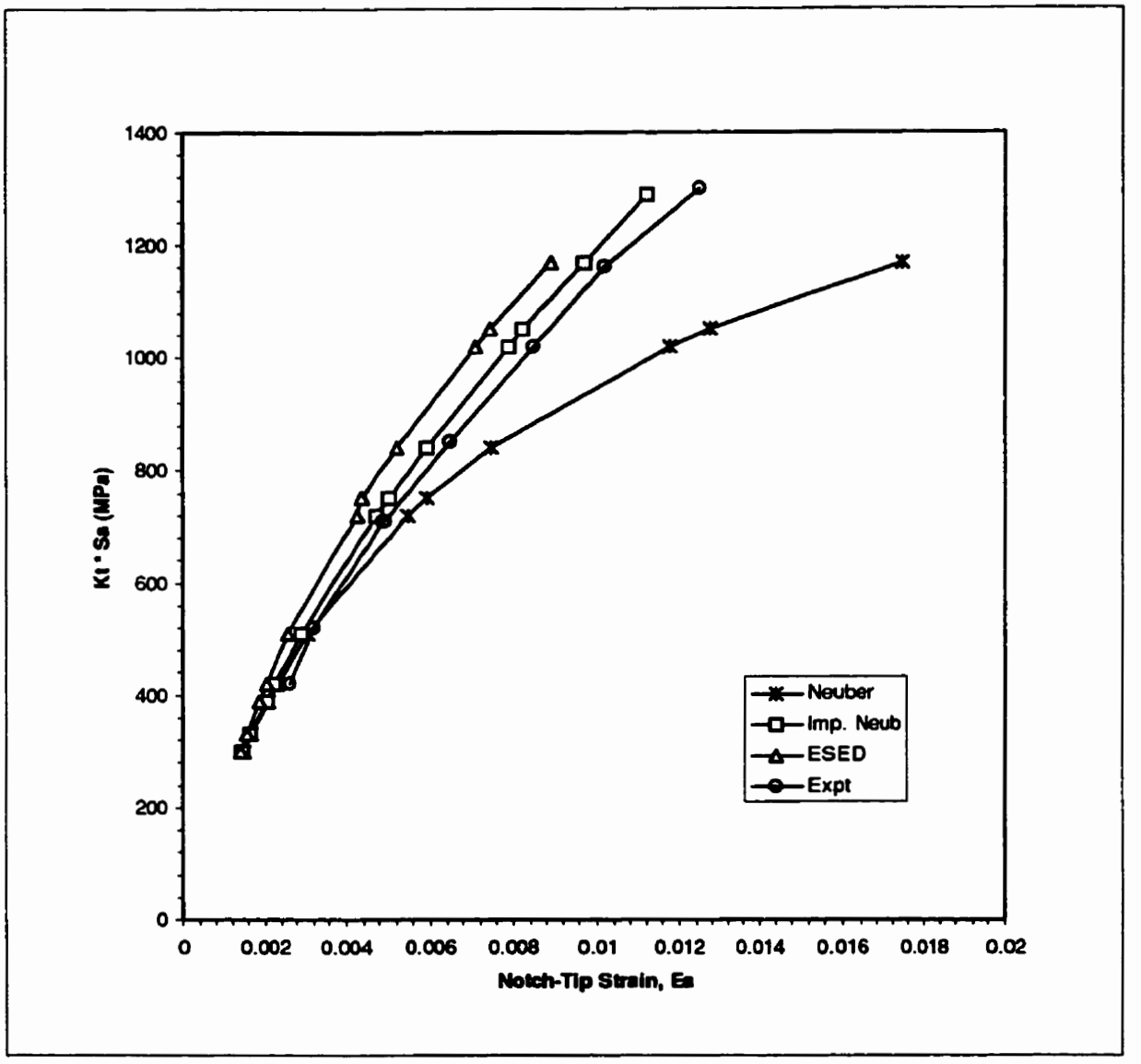

Figure 4.6 : Calculated and experimental Notch-tip strains in a keyhole SAE Compact tension specimen under cyclic loading for MAN-TEN Steel under *Plane strain* conditions

Figures 4.3 and 4.4 show a comparative notch-tip strain estimates, under plane stress conditions. It is found that the energy approach as well as the improved Neuber's rule, overestimates the notch-tip strains. This can be attributed to the fact that the plane stress conditions do not exist near the notch-tip of an SAE compact tension keyhole specimen. The plane stress assumption is frequently used in the industry and is found to be very useful in simplifying the complex state of stress in mechanical components. In the present work, an effort was made to evaluate the local stress-strain methods under plane stress conditions, even though these conditions do not exist at the notch-tip.

Results shown in figures 4.5 and 4.6 for RQC-100 and MAN-TEN, respectively, are under plane strain conditions. Estimates of energy approach and improved Neuber's rule, for a nominal stress range within $0 \leq S_a \leq \sigma_{ys}$, are found to be in good agreement with the experimental values. Further it can be noted that energy approach *underestimated* the notch-tip strains by a very small amount.

Figures 4.7 to 4.8 present the comparison of fatigue crack initiation life estimates using the three local stress-strain methods for different load levels under plane stress and plane strain conditions.

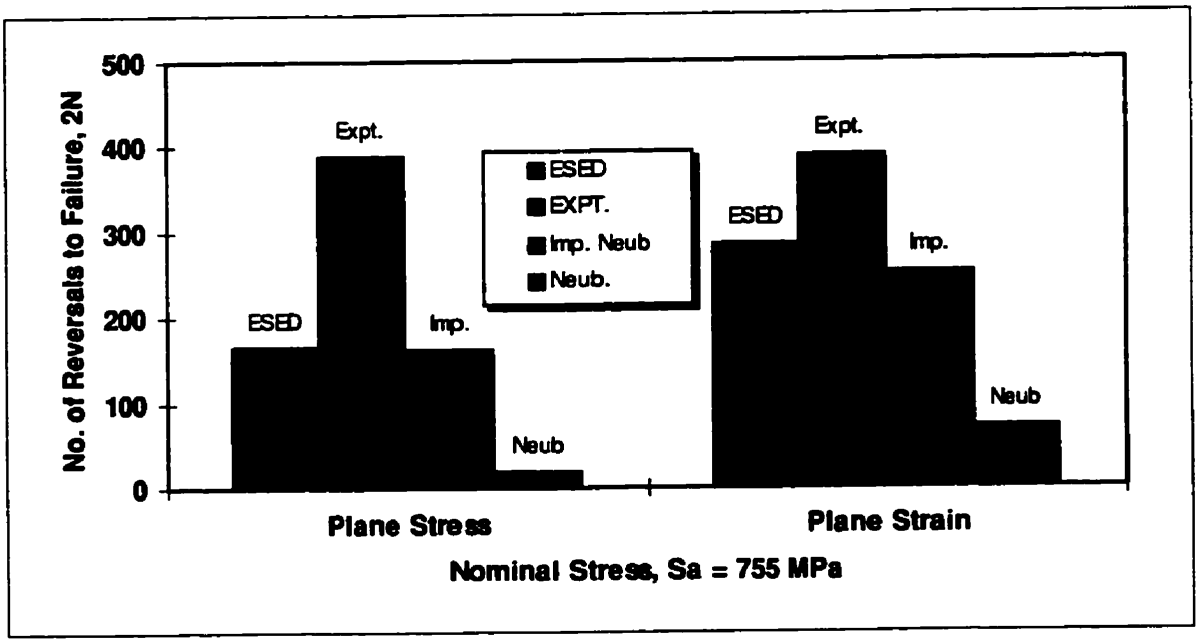

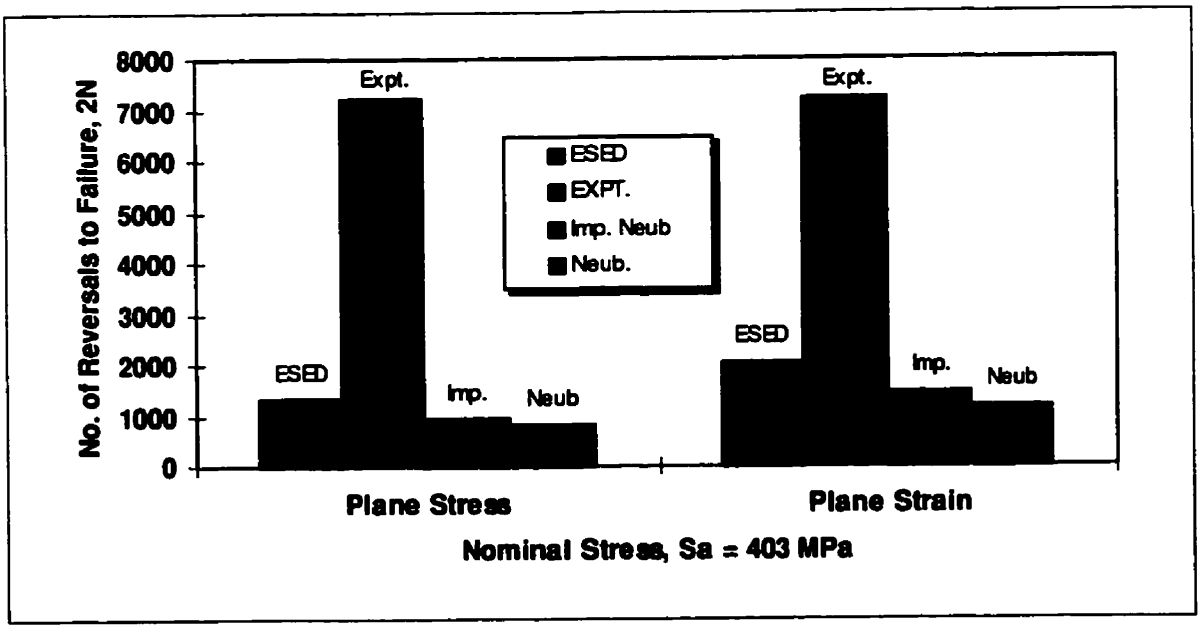

Figure 4.7 : Comparison of Fatigue initiation life predictions with experimental results for RQC-100 Steel, keyhole specimen

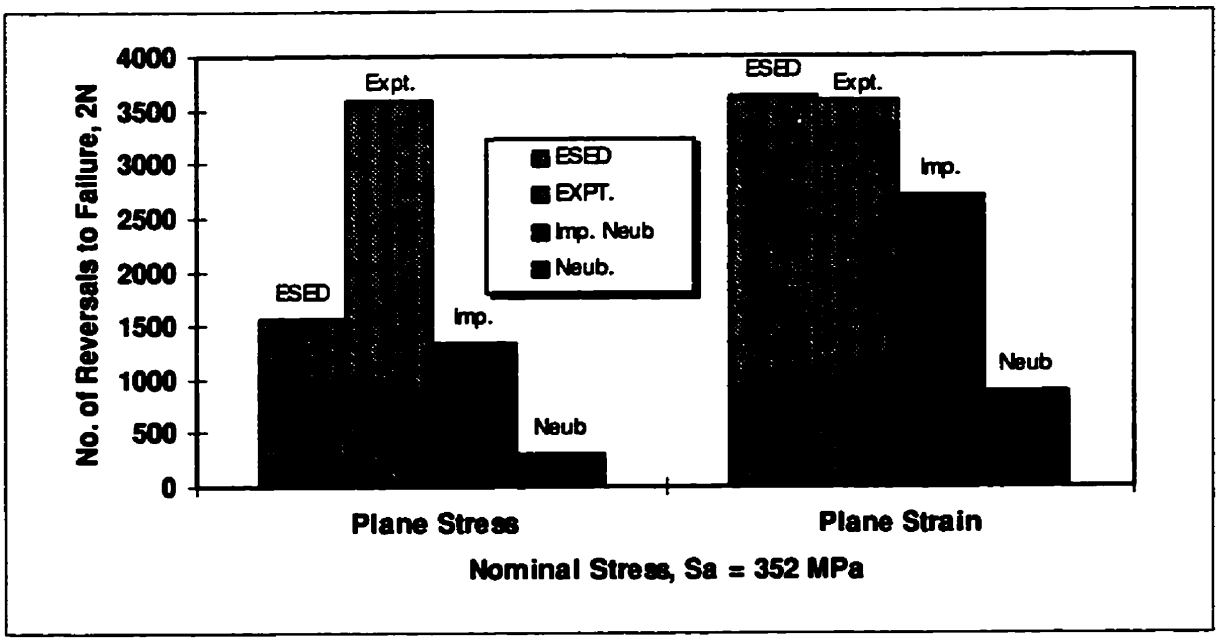

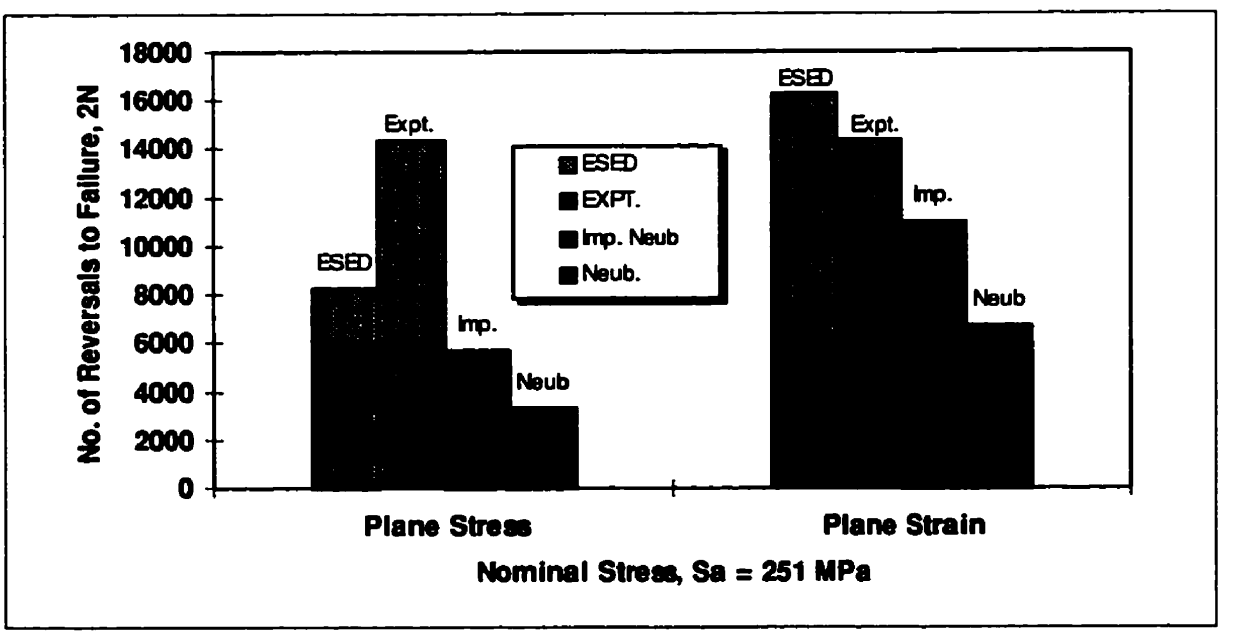

Figure 4.8 : Comparison of Fatigue initiation life predictions with experimental results for MAN-TEN Steel, keyhole specimen

the strains are accurate. Due to its exponential nature, the life estimates are highly sensitive to the accuracy of notch tip strain calculations. Therefore the fatigue life estimation capabilities of local stress-strain methods depend on their strain estimates.

As can be seen, the notch-tip strains by the energy approach as well as the improved Neuber's rule, in plane strain conditions are in good agreement with the experimental results. For MAN-TEN steel the strains are found to be slightly underestimated. This is due to the idealistic assumption of pure plane strain state near the notch-tip in the present study. But, in fact, the keyhole specimen behaves in an intermediate manner, *i.e.* between plane stress and plane strain, where the biaxiality as reported by Dowling [6], is a little less pronounced than what it would have been in a pure plane strain state. This phenomena leads to the slight underestimation of notch-tip strains under plane strain conditions.

Basically, the energy approach and Neuber's rule are the same in the elastic range. But, in the case of localized plasticity, Neuber's rule no longer represents the strain energy density due to the local elastic-plastic stress-strain field, leading to huge discrepancies in the calculated and measured notch-tip strains. This is due to the approximate nature of Neuber's rule , where the exponents of K_σ and K_ε are fixed as 0.5 for all materials. This is generally not true; instead the exponents are found to be a function of cyclic material properties. The improved Neuber's rule incorporated a parameter 'm', which is directly proportional to n' and inversely proportional to K'/E, and this has considerably reduced the approximate nature of the conventional Neuber's rule.

Unfortunately the notch-tip strain estimates obtained by the improved Neuber's rule are not as good as those of energy approach. Nevertheless, the fatigue life estimates obtained by using a simpler approach such as the improved Neuber's rule with reasonably accuracy [within 15 to 20% of ESED results] can functionally replace the most widely used, conventional Neuber's rule.

Chapter Five

CONCLUSIONS AND RECOMMENDATIONS

5.1 Conclusions

An evaluation of three local stress-strain methods has been presented. Each method is analyzed in plane stress as well as in plane strain conditions under cyclic loading.

A standard keyhole SAE compact tension specimen made out of two commercial automotive steels, RQC-100 and MAN-TEN has been used in this evaluation.

The results obtained through the local stress-strain methods have been compared with the published values of measured notch-tip strains and fatigue initiation life.

It is found that Neuber's rule overestimates the notch-tip stresses and strains in both materials under plane stress as well as plane strain conditions. Further, the fatigue initiation life estimates based on Neuber's method are highly conservative.

When compared to the experimental results, the notch-tip strains and fatigue life estimates based on the ESED method, up to the general yielding range, are found to be the best under plane stress and plane strain conditions.

The improved Neuber's rule estimates strains as well as fatigue life far better than the Neuber's rule. The strain estimates are found to be within a range of 10 to 12% and the fatigue life estimates are within 15 to 20% of the corresponding energy approach estimates.

Based on the above observation, it is suggested that the improved Neuber's rule can effectively replace the conventional Neuber's rule. Further, it does not require any major modifications in the current procedures, such as estimation of plastic zone and a plastic zone correction parameter as seen to be necessary in the energy approach. Therefore the improved Neuber's rule can be used for efficient fatigue life estimates in place of intricate ESED method.

5.2 Recommendations for Further Research

The present evaluation is carried out under cyclic axial loading. The ESED method and improved Neuber's rule are equally valid for bending as well. A study using cyclic bending or a combination of axial and bending loading can provide better insight in real life situations. However, it should be noted that the ESED method has not yet been verified for torsional loading.

Similar evaluation of local stress-strain methods for aluminum alloys would be of great importance for studying fatigue failures related to the aircraft industry. Experimental work need to be done to study the aluminum alloys behavior under cyclic loading.

REFERENCES

[1] J.F. Taverneli and L.F. Coffin, Jr., "Experimental Support for Generalized Equation Predicting Low Cycle Fatigue," *Trans.* ASME, *Journal of Basic Engineering*, Vol. 84, No. 4, p. 533, Dec. 1962.

[2] S.S. Manson, discussion of reference [1], *Trans.* ASME, *Journal of Basic Engineering*, Vol. 84, No. 4, p. 537, Dec. 1962.

[3] Fatigue Under Complex Loading: Analysis and Experiments, ed. R.M. Wetzel. SAE. Warrendale, PA, 1977.

[4] Ramberg, W. and Osgood, W.R., NACA Technical Note 902, National Advisory Committee for Aeronautics, Washington, D.C., 1943.

[5] N.E. Dowling, "Notched Member Fatigue Life Predictions combining Crack Initiation and Propagation," *Fatigue of Engineering Materials and Structures*, Vol.2, No.2, pp. 129 -138, 1979.

[6] Dowling, N.E., Brose, W.R. and Wilson, W.K., "Notched Member Fatigue Life Predictions by the Local Strain Approach," *Fatigue Under Complex Loading : Analysis and Experiments*, Society for Automotive Engineers, Warrendale, PA, 55-84, 1977.

[7] "Wöhler's Experiments on the Strength of Metals," Engineering, August 23, p.160, 1967.

[8] Mann, J.Y., "The Historical Developments of Research on the Fatigue of Materials and Structures," *The Journal of the Australian Institute of Metals*, pp. 222-241, Nov. 1958.

[9] Endo, T. and Morrow, JoDean, "Cyclic Stress-Strain and Fatigue behavior of Representative Aircraft Metals," Journal of Materials, JMLSA, Vol. 4, No. 1, March 1969, pp. 159-175.

[10] Topper, T.H., Wetzel, R.M. and Morrow, J. " Neuber's rule applied to fatigue notched specimens", *Journal of Materials*, Vol. 4, No. 1, 1969, pp. 200-209.

[11] Zhang, D. and Sandor, B.I., "Low-Cycle Fatigue Analysis of Notched members," Journal of Testing and Evaluation, JTEVA, Vol. 17, No. 4, July 1989, pp. 212-217.

[12] Bela I. Sandor, "Fundamentals of Cyclic Stress Strain," The University of Wisconsin Press, Wisconsin, 1972.

[13] Socie, D.F., Dowling, N.E., and Kurath, P., "Fatigue Life Estimation of Notched Members," Fracture Mechanics : Fifteenth Symposium, ASTM STP 833, R.J. Sanford, Ed., ASTM, Philadelphia, pp. 284-299, 1984.

[14] Neuber, H., " Theory of Stress Concentration for Shear-strained Prismatical Bodies with Arbitrary Non-linear Stress-strain Law", *Journal of Applied Mechanics*, Vol. 28, No. 4, 161, pp. 544-550, 1961.

[15] B. N. Leis, C.V.B. Gowda and T.H. Topper, "Some Studies of the Influence of Localized and Gross Plasticity on the Monotonic and Cyclic concentration Factors," *Journal of Testing and Evaluation*, 1, 341-348, 1973.

[16] Conle, A. and Nowack, H., " A Verification of a Neuber-based Notched Analysis by the Companion Specimen Method," *Experimental Mechanics*, 17 (2), 53-63 , 1977.

[17] T. Seeger and P. Heuler, "Generalized application of Neuber's rule," *Journal of Testing and Evaluation*, 8, 199-204, 1980.

[18] J.W. Hutchinson, "Singular behavior at the end of a tensile crack in a hardening material", *Journal of Mech. Phys. Solids* 16, 13-31, 1968.

[19] T.J. Walker, " A quantitative strain-and stress state criterion for failure in the vicinity of sharp cracks," *Nuclear Technology*, 23, 189-203, 1974.

[20] K. Molski and G. Glinka, "A Method of Elastic-Plastic Stress and Strain Calculation at a Notch Root," *Material Science Engineering*, 50, 93-100, 1981.

[21] Glinka, G., "Calculation of Inelastic Notch-tip Strain-stress Histories Under Cyclic Loading," *Engineering Fracture Mechanics*, 2 (5), 839-954, 1986.

[22] Wu, Y.-S., "The improved Neuber's rule and low cycle fatigue life estimation", *Low Cycle Fatigue*, ASTM STP 942, American Society for Testing and Materials, Philadelphia, 1988, pp. 1007-1021.

[23] L. Tucker and S. Bussa, "The SAE Cumulative Fatigue Damage Test Program," *Fatigue Under Complex Loading : Analysis and Experiments*, Society for Automotive Engineers, pp. 1, 1977.

[24] Mowbray, D.F. and McConnolee, J.E., "Application of finite element stress analysis and stress-strain properties in determining notch fatigue specimen deformation and life," in *Cyclic Stress-Strain Behavior-Analysis, Experimentation and Failure Prediction*, ASTM STP 519, American Society for Testing and Materials, Philadelphia, pp. 151-169, 1973.

[25] Coulon, A., Knosp, B. and Saisse, M., "Plastic Strain Arising from Fatigue Crack Initiation," *Journal of Testing and Evaluation*, 13 (4), 265-274, 1985.

[26] Irwin, G.R., " Linear Fracture Mechanics, Fracture Transition and Fracture Control," *Engineering Fracture Mechanics*, 1 (2), 241-257, 1968.

[27] Glinka, G and Newport, A., "Effect of notch-strain calculation method on fatigue crack initiation life predictions", *Experimental Mechanics*, Vol. 30, June 1990, pp. 208-216.

[28] Glinka, G., Ott, W. and Nowack, H., "Elasto-plastic Plane Strain Analysis of stress and Strains at the Notch Root," *Journal of Engineering materials and Technology*, 110 (3), 195-204, 1988.

[29] Bannentine J., "Fundamentals of Metal Fatigue," John Wiley & sons, Inc., New York, 1980.

[30] H.O. Fuchs and R.I. Stephens, "Metals Fatigue in Engineering," John Wiley & sons, Inc., New York, 1980.

[31] "Technical Report on Fatigue Properties," SAE J1099, 1975.

[32] Morrow, J. D., "Cyclic Plastic Strain Energy and Fatigue of Metals," in *Internal Friction, Damping, and Cyclic Plasticity, ASTM STP 378*, American Society for Testing and Materials, Philadelphia, pp. 45-87, 1965.

[33] ASTM E 606-77T: "Tentative Recommended Practice for Constant Amplitude Low-Cycle Fatigue Testing," *American Society for Testing and Materials*, ASTM Standards, 1977.

[34] Bignonnet, A. and Buthod-Cuan, H., "Armorcage en fatigue of partir d'une entaille," *Strength of Metals and Alloys*, Proc. 7th Int. Conf. on the Strength of Metals and Alloys, Pergamon Press, 1985, pp. 1231-1236.

Appendix A

Computer Code

The following is a Computer code in 'C' language, to perform the necessary iterative calculations in analytically estimating the notch-tip stress-strains and the fatigue crack initiation life:

(*Note:* Edit this program appropriately for plane stress and plane strain condition.)

```
#include <stdio.h>
#include <stdlib.h>
#include <math.h>
#include <string.h>
#include <ctype.h>

double tolerance;
double neuber(double x);
double impneuber(double x);
double ESED(double x);
double Pzone_size(double x);

void swap_double(double *a, double *b);
```

```
double bisection(double (*function)(double),double low, double high);
double calc_eps(double x);

#define max(A,B) (A >= B ? A : B)

void func(double guess, double *val, double *der, double eps);
double calc_guess(double eps);
double newton(double guess, double eps);

double sf,sm,E,b,ef,c;
double sigamp, sigmax;
double epsamp, epsmax;
double samp, smax;
double cycles, reversals;
char *output_file;
char *input_file;
FILE *ifile, *ofile;

double K;
double n;
double S;
double Kt;
double n_rad;
double a;
double m, j;
double Cp;
double rp;
double sigys;

int main(int argc, char *argv[])
```

```
{
        int i, iter_mat, iter_not;
        output_file = NULL;
        input_file = NULL;

        for (i=1 ; i < argc ; i++)
        {
                if (strcmp(argv[i],"-o") == 0)
                        output_file = strdup(argv[i+1]);
                if (strcmp(argv[i],"-i") == 0)
                        input_file = strdup(argv[i+1]);
                if (strcmp(argv[i],"-tolerance") == 0)
                        tolerance = atof(argv[i+1]);
                if (strcmp(argv[i],"-h") == 0)
                {
                        printf("Usage %s -o [output_file] -i [input_file] -
tolerance\n",argv[0]);
                        exit(0);
                }
        }

        if (input_file != NULL)
                ifile = fopen(input_file,"r");
        else
                ifile = stdin;

        if (output_file != NULL)
                ofile = fopen(output_file,"a");
        else
                ofile = stdout;
```

```
        setbuf(ofile,NULL);

/* Iterating for different materials and  notch geometries by changing the 'iter_mat' */

        for( iter_mat = 1; iter_mat <= 1; iter_mat ++ )
        {

/* The following Cyclic Stress-Strain and Strain-Life constants are to be entered for the
material under study */

                printf("Enter E (MPa) :");
                scanf("%lf",&E);

                printf("Enter Yield Strength (MPa) :");
                scanf("%lf",&sigys);

                printf("Enter K (MPa) :");
                scanf("%lf",&K);

                printf("Enter n :");
                scanf("%lf",&n);

                printf("Enter sf :");
                scanf("%lf",&sf);

                printf("Enter b :");
                scanf("%lf",&b);

                printf("Enter ef :");
```

```
        scanf("%lf",&ef);

        printf("Enter c :");
        scanf("%lf",&c);

/* Enter Notch parameters */

        printf("Enter Peterson parameter, a  :");
        scanf("%lf",&a);

        printf("Enter Tolerance :");
        scanf("%lf",&tolerance);

        fprintf(ofile,"E = %6.3f\n",E);
        fprintf(ofile,"K = %6.3f\n",K);
        fprintf(ofile,"n = %6.3f\n",n);
        fprintf(ofile,"sf = %6.3f\n",sf);
        fprintf(ofile,"b = %6.3f\n",b);
        fprintf(ofile,"ef = %6.3f\n",ef);
        fprintf(ofile,"c = %6.3f\n",c);
        fprintf(ofile,"a = %6.5f\n",a);
        fprintf(ofile,"Tolerance = %10.6f\n",tolerance);

        for( iter_not = 1; iter_not <= 1; iter_not ++ )
        {

                printf("Enter Kt  :");
                scanf("%lf",&Kt);

                printf("Enter notch radius  :");
```

```
                scanf("%lf",&n_rad);

                fprintf(ofile,"Kt = %6.3f\n",Kt);
                fprintf(ofile,"Notch-tip radius = %6.5f\n\n",n_rad);

                /* Assign the loading range in the loop below */

                for(samp = 100, smax = samp; samp <= 800; samp = samp + 10,
smax = smax + 10 )
                {
                        /* USING NEUBER'S RULE */

                        S=samp;
                        sigamp = bisection(neuber,0.0,10000.0);
                        epsamp = calc_eps(sigamp);
                        S=smax;
                        sigmax = bisection(neuber,0.0,10000.0);
                        epsmax = calc_eps(sigmax);
                        sm = sigmax-sigamp;

                        fprintf(ofile,"S_amp = %6.1f\n",samp);
                        fprintf(ofile,"S_max = %6.1f\n",smax);

                        fprintf(ofile,"Using Neuber's Rule\n\n");
                        fprintf(ofile,"sigamp = %6.1f\n",sigamp);
                        fprintf(ofile,"sigmax = %6.1f\n",sigmax);
                        fprintf(ofile,"epsamp = %6.5f\n",epsamp);
                        fprintf(ofile,"epsmax = %6.5f\n",epsmax);
                        cycles = newton(calc_guess(epsamp),epsamp);
                        reversals = 2 * cycles;
```

```
                    fprintf(ofile,"REVERSALS TO FAILURE, 2Nf =
%6.0f\n",reversals);

                    fprintf(ofile,"\n\n");

                    /* USING IMPROVED NEUBER'S RULE */

                    S=samp;
                    sigamp = bisection(impneuber,0.0,10000.0);
                    epsamp = calc_eps(sigamp);
                    S=smax;
                    sigmax = bisection(impneuber,0.0,10000.0);
                    epsmax = calc_eps(sigmax);
                    sm = sigmax-sigamp;

                    fprintf(ofile,"Using Improved Neuber's Rule\n\n");
                    fprintf(ofile,"sigamp = %6.1f\n",sigamp);
                    fprintf(ofile,"sigmax = %6.1f\n",sigmax);
                    fprintf(ofile,"epsamp = %6.5f\n",epsamp);
                    fprintf(ofile,"epsmax = %6.5f\n",epsmax);
                    cycles = newton(calc_guess(epsamp),epsamp);
                    reversals = 2 * cycles;
                    fprintf(ofile,"REVERSALS TO FAILURE, 2Nf =
%6.0f\n",reversals);

                    fprintf(ofile,"\n\n");

                    /* USING 'ESED' METHOD */

                    S=samp;
                    sigamp = bisection(ESED,0.0,10000.0);
                    epsamp = calc_eps(sigamp);
```

```
                    S=smax;
                    sigmax = bisection(ESED,0.0,10000.0);
                    epsmax = calc_eps(sigmax);
                    sm = sigmax-sigamp;

                    fprintf(ofile,"Using ESED Method\n\n");
                    fprintf(ofile,"sigamp = %6.1f\n",sigamp);
                    fprintf(ofile,"sigmax = %6.1f\n",sigmax);
                    fprintf(ofile,"epsamp = %6.5f\n",epsamp);
                    fprintf(ofile,"epsmax = %6.5f\n",epsmax);
                    cycles = newton(calc_guess(epsamp),epsamp);
                    reversals = 2 * cycles;
                    fprintf(ofile,"REVERSALS TO FAILURE, 2Nf =
%6.0f\n",reversals);
                    fprintf(ofile,"----------\n\n");


                }   /* End of 'for loop' for samp  */

            }   /* End of 'for loop' for Notch iteration */

        }   /* End of 'for loop' for Material iteration */

}

/* The Functions */

double neuber(double x)
{
        double temp,ss;
```

```
ss = ((S/E) + (pow((S/K),(1.0/n))));
temp = (((x/2.0)*((x/E) + (pow((x/K),(1.0/n))))) - (pow(Kt,2.0)*S*ss/2.0));
        return(temp);
}

double ESED(double x)
{
        double temp,i;
        double z, Cp,rp;

/* Provide an approximate range for the plastic zone size */

        rp = bisection(Pzone_size,3.0,0.001);
        if ((n_rad/rp) > 2.0)
        {
                rp = n_rad/2.0;
                Cp = 1.0;
        }
        else
        {
                z = n_rad/rp;
                Cp = ((2.0 - 0.5*z + 0.25*z*z)/(1.0 + 0.5*z));
        }

/* Since, Cp is required only when Rho/rp <= 2 , else Cp =1; Ref.[20] */

/* The function remains same for plane stress as well as plane strain conditions */

        i = 1.0 + (1.0/n);
```

```
        temp=((pow(x,2.0)/(2.0*E))+((pow(x,i))/((n+1.0)*(pow(K,(1.0/n)))))-
(Cp*(pow((Kt*S),2.0))/(E*2.0)));

        return(temp);

}

double impneuber(double x)
{
        double temp, i, j, m, ss1;

/* The following function is under plane stress conditions */

m = 0.48 + 0.31*n - 8.6*K/E;

/* The following function is under plane strain conditions */

m = 0.42 +0.25*n - 3.92*K/E;

        i = 1.0/(1.0-m);
        j = m/(1.0-m);

temp = ((x/E)+(pow((x/K), (1.0/n)))-((pow((Kt*S), i))/((pow(x, j))*E)));

        return(temp);
}
```

/* The Bisection method */

```
double bisection(double (*function)(double), double low, double high)
{

        double mid;
        double temp;
        double temp1,temp2;

        mid = (low+high)/2.0;
        temp = function(mid);
        temp1 = function(low);
        temp2 = function(high);

        if ((fabs(temp) <= tolerance))
                return(mid);
        else
        {
                if ((temp*temp2) > 0.0)
                        swap_double(&high, &mid);
                if ((temp*temp1) > 0.0)
                        swap_double(&low, &mid);

                return(bisection(function, low, high));
        }
}


void swap_double(double *a, double *b)
{
        double temp;
```

```
        temp = *a;
        *a = *b;
        *b = temp;
        return;
}
/* The function to estimate the plastic zone size  -- from Ref.[21]  */
/* Under Plane Stress */

double Pzone_size(double x)
{
        double temp;
        temp = ((n_rad/x)+(0.75*pow((n_rad/x),3.0))-pow(((2.818*sigys)/(Kt*S)),2.0));
        return(temp);
}

/* Under Plane Strain */

double Pzone_size(double x)
{
        double temp;
        temp = ((n_rad/x) )*(pow((1.0-(2.0*0.3)),2.0))+(0.75*pow((n_rad/x),3.0))-
pow(((2.818*sigys)/(Kt*S)),2.0));
        return(temp);
}


/* Calculation of notch-tip strains, using the notch-tip stress in the stress-strain relation */
double calc_eps(double x)
{
        double temp;
```

```
        temp=(x/E)+pow((x/K),(1.0/n));
        return(temp);
}

/* Estimation of Reversals to Failure -- Newton's Method */

double newton(double guess, double eps)
{

        double dx,val,der;

        func(guess,&val,&der, eps);
        dx = val/der;
        guess = guess-dx;
        if (fabs(dx) <= tolerance)
                return(guess);
        else
                return(newton(guess,eps));
}

void func(double guess, double *val, double *der, double eps)
{
        *val = ((sf-sm)*(pow(2.0*guess,b))/E) + (ef*(pow(2.0*guess,c))) - eps;
        *der = ((sf-sm)*b*2.0*(pow(2.0*guess,(b-1)))/E) + (ef*c*2.0*(pow(2.0*guess,(c-
1))));
}

/* To estimate the initial guess required by the Newton's method */

double calc_guess(double eps)
```

```
{
        double Nf1;
        double Nf2;

        Nf1 =(0.5*(pow(((eps*E)/(sf-sm)),(1.0/b))));
        Nf2 =(0.5*(pow(((eps)/ef),(1.0/c))));

        return(max(Nf1,Nf2));
}
```

Appendix B

Sample Calculation

A sample calculation is illustrated for better insight in the analytical calculations.

Choose $S_a = 400$ MPa, for RQC-100 Steel.
Please refer to the tables 4.1 to 4.4 for the cyclic material and fatigue properties along with the notch parameters for RQC-100 Steel.

Notch-tip stresses and strains and fatigue crack initiation life calculations using :

1. Neuber's Rule

Under Plane Stress:
Substitute the appropriate values in equations (3.4) and (3.6), which are listed below for convenience.

$$\sigma_a \varepsilon_a = \frac{(K_t S_a)^2}{E} \tag{3.4}$$

$$\varepsilon_a = \frac{\sigma_a}{E} + \left(\frac{\sigma_a}{K'}\right)^{1/n'} \tag{3.6}$$

we have,

$$\sigma_a \varepsilon_a = \frac{(3*400)^2}{203000} = 7.0936$$

$$\varepsilon_a = \frac{7.0936}{\sigma_a}$$

Introducing ε_a in equation (3.6)

$$\frac{7.0936}{\sigma_a} = \frac{\sigma_a}{203000} + \left(\frac{\sigma_a}{1150}\right)^{1/0.1} \qquad \text{(B.1)}$$

The above relation (B.1) is a non-linear equation in σ_a. It is difficult to solve analytically, but a numerical method such as bisection method can easily solve it.

By solving equation (B.1) using bisection method with the aid of computer code, listed in appendix A,

$$\sigma_a = 698.6 \text{ MPa}$$

Substituting σ_a in equation (3.6)

$$\varepsilon_a = 0.01029$$

By introducing the computed ε_a and the appropriate fatigue properties in Coffin -Manson relation,

$$\varepsilon_a = \frac{\sigma'_f - \sigma_m}{E}(2N)^b + \varepsilon'_f (2N)^c$$

and solving for the number of reversals (2N) to failure, using the computer code, we have

Number of reversals to failure, 2N = 835 (Plane stress)

Note that $\sigma_m = 0$, since the applied loading is completely reversed (R = -1).

Under plane strain:

The procedure involved here is same as in the plane stress, but the appropriate cyclic material properties in plane strain condition shall be used instead.

$$\sigma^*_a \varepsilon^*_a = \frac{(3*400)^2}{203000}\left(1-(0.3)^2\right)$$

$$\varepsilon^*_a = \frac{6.455}{\sigma^*_a}$$

Introducing ε^*_a in equation (3.12)

$$\frac{6.455}{\sigma^*_a} = \frac{\sigma^*_a}{203000}\left(1-(0.3)^2\right)+\left(\frac{\sigma^*_a}{1343.65}\right)^{1/0.1017}$$

$$\sigma^*_a = 780.7 \text{ MPa}$$

Substituting σ^*_a in equation (3.9)

$$\varepsilon^*_a = 0.00830$$

By introducing the computed ε^*_a and the appropriate fatigue properties in Coffin-Manson relation, and solving for the number of reversals (2N) to failure, using the computer code, we have

Number of reversals to failure, 2N = 1191 (Plane strain)

2. Improved Neuber's rule

Under plane stress:

$m = 0.48 + 0.31\, n' - 8.60\, K'/E$ in plane stress condition. (3.10)

After proper substitutions,

m =0.46

Introducing m =0.46 and other values in equation (3.15), we have a non-linear equation in σ_a, which can be solved by the computer code.

$$\frac{\sigma_a}{E}+\left(\frac{\sigma_a}{K'}\right)^{1/n'} = \left(\frac{K_t S_a}{E^{1-m}\sigma_a^{\,m}}\right)^{1/1-m} \qquad (3.15)$$

$$\frac{\sigma_a}{203000}+\left(\frac{\sigma_a}{1150}\right)^{1/0.1}=\left(\frac{3.0*400}{(203000)^{1-0.46}\sigma_a^{0.46}}\right)^{1/1-0.46}$$

$$\sigma_a = 690.6 \text{ MPa}$$

Substituting back in the uniaxial material stress-strain curve,

$$\varepsilon_a = 0.0095$$

From Coffin-Manson relation, we have

Number of reversals to failure, 2N = 974 (Plane stress)

Under plane strain:

$m = 0.42 + 0.25\, n^* - 3.92\, K^*/E^*$ in the plane strain condition. (3.11)

m =0.42

Using equations (2.12) and (3.16), with plain strain material properties (E^*, K^*, n^*), we have

$$\sigma^*_a = 766.6 \text{ MPa}$$

and

$$\varepsilon^*_a = 0.00746$$

By introducing the computed ε^*_a and the appropriate fatigue properties in Coffin-Manson relation, and solving for the number of reversals (2N) to failure, using the computer code, we have

Number of reversals to failure, 2N = 1482 (Plane strain)

3. Using ESED method

We need to now know the plastic zone size prior to the estimation of C_p or the notch-tip strain.

Under plane stress:

As the notch-tip radius is known (from the notch geometry), we need to solve for r_p in equation (3.20).

$$\sigma_{ys} = \frac{K_t S_a}{2\sqrt{2}}\left[\frac{\rho}{r_p} + \frac{3}{4}\left(\frac{\rho}{r_p}\right)^3\right]^{1/2} \tag{3.20}$$

Making appropriate substitutions and solving for r_p using bisection method,

$$620 = \frac{3*400}{2\sqrt{2}}\left[\frac{0.187}{r_p} + \frac{3}{4}\left(\frac{0.187}{r_p}\right)^3\right]^{1/2}$$

r_p = 0.169 inches

Therefore, C_p = 1.129

Using C_p and the uniaxial properties in equation (3.25) and solving for σ_a, we have

$$\frac{C_p(K_t S_a)^2}{2E} = \frac{\sigma_a^2}{2E} + \frac{\sigma_a}{n'+1}\left(\frac{\sigma_a}{K'}\right)^{1/n'} \tag{3.25}$$

$$\frac{1.129(3*400)^2}{2*203000} = \frac{\sigma_a^2}{2*203000} + \frac{\sigma_a}{0.1+1}\left(\frac{\sigma_a}{1150}\right)^{1/0.1}$$

$$\sigma_a = 673.1 \text{ MPa}$$

Substituting back in the uniaxial material stress-strain curve,

$$\varepsilon_a = 0.00803$$

From Coffin-Manson relation, we have

Number of reversals to failure, 2N = 1374 (Plane stress)

Under plane strain:

The above procedure is repeated with plane strain material properties and biaxial stress-strain curve in place of the uniaxial properties of stress-strain curve.

Making appropriate substitutions in equation (3.21) and solving for r_p^* using bisection method,

$$720 = \frac{3*400}{2\sqrt{2}}\left[\frac{0.187}{r^*_p} + \frac{3}{4}\left(\frac{0.187}{r^*_p}\right)^3\right]^{1/2} \qquad \upsilon = 0.3;$$

r^*_p = 0.1233 inches

Therefore, C^*_p = 1.033

Using C^*_p and the biaxial properties in equation (3.27) and solving for σ^*_a, we have

$$\frac{C^*_p(K_t S_a)^2}{2E^*} = \frac{(\sigma^*_a)^2}{2E^*} + \frac{\sigma^*_a}{n^*+1}\left(\frac{\sigma^*_a}{K^*}\right)^{1/n^*} \qquad (3.27)$$

$$\frac{1.033(3*400)^2}{2*223077} = \frac{(\sigma^*_a)^2}{2*223077} + \frac{\sigma^*_a}{0.1017+1}\left(\frac{\sigma^*_a}{1343.65}\right)^{1/0.1017}$$

$$\sigma^*_a = 746 \text{ MPa}$$

Substituting back in the material stress-strain curve,

$$\varepsilon^*_a = 0.00643$$

By introducing the computed ε^*_a and the appropriate fatigue properties in Coffin - Manson relation, and solving for the number of reversals (2N) to failure, using the computer code, we have

Number of reversals to failure, 2N = 2051 (Plane strain)

Appendix C

Derivation of Loading Equation (2.13)

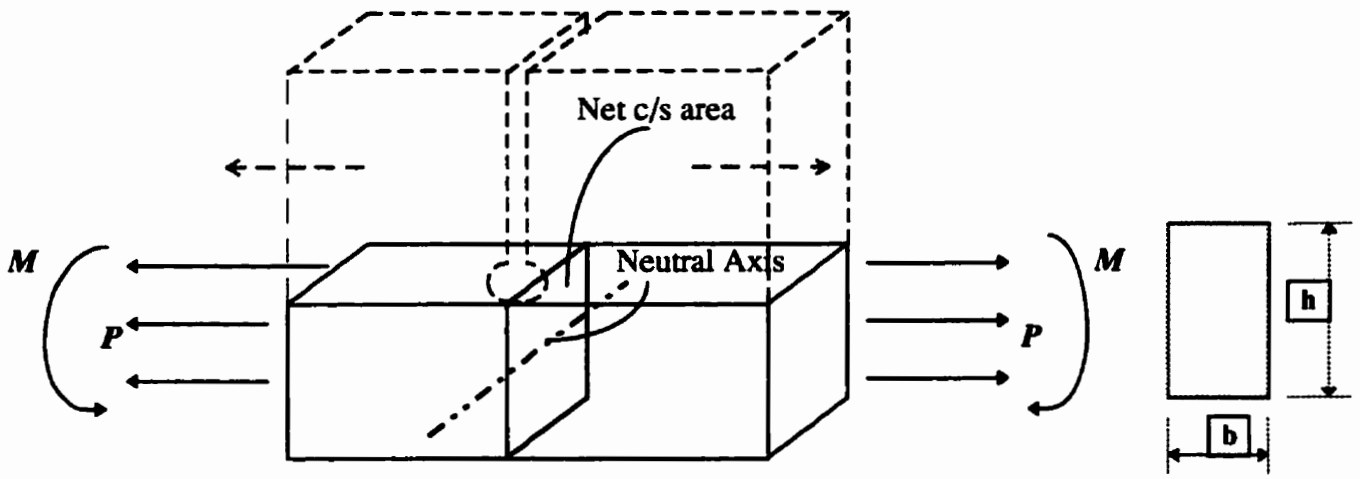

Figure C-1: Net section of SAE keyhole specimen

Thickness $b = 9.5\ mm$

Height of the net section, $h = 63.85\ mm$

$$z = \frac{h}{2} = \frac{63.85}{2} = 31.925mm$$

Distance between the force center line and the center line of the net section,

$$l = \frac{(68.6 - 4.75)}{2} + 4.75 + 25.4 = 62.075mm$$

Net cross-sectional area, $A = b * h = 9.5 * 63.85 = 606.575\ mm$

Moment about the neutral axis of the net section, $M = P * l = 62.075\ P$

Moment of inertia, $I = \frac{bh^3}{12} = \frac{(9.5)(63.85)^3}{12} = 206074.88mm^4$

Nominal stress, $S_a = \frac{Mz}{I} + \frac{P}{A}$

$$S_a = \frac{(62.075P) * (31.925)}{206074.88} + \frac{P}{606.575}$$

$$= 0.011265\ P\ \frac{force\ units}{mm^2}$$

$$= 11.265P$$

where P in kN and S_a in MPa.

IMAGE EVALUATION TEST TARGET (QA-3)

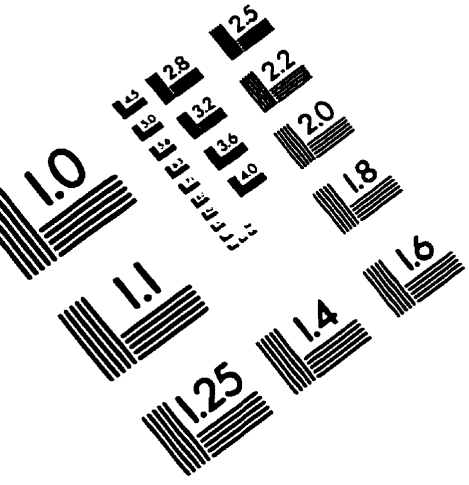

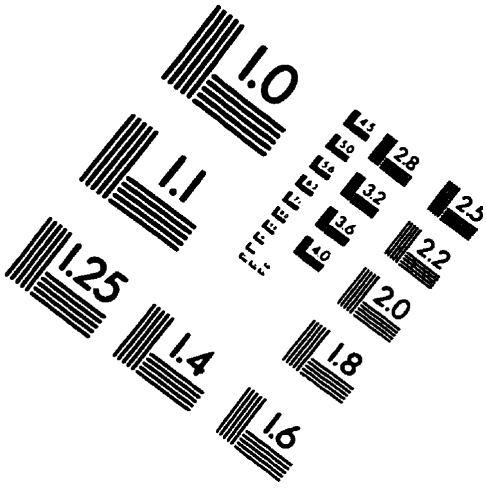

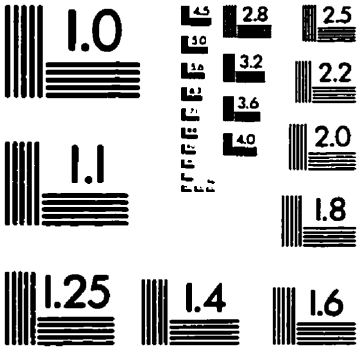

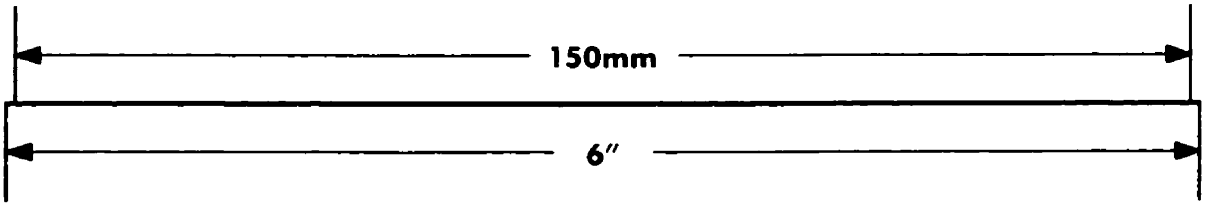

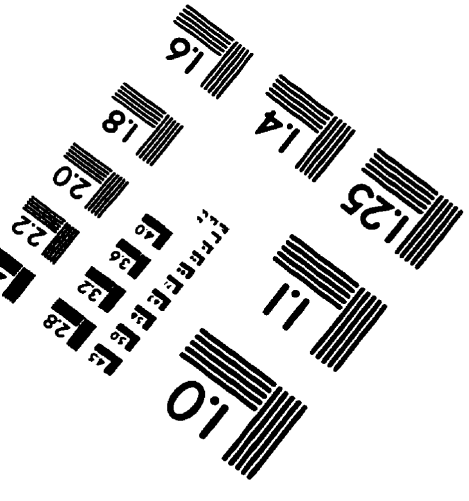

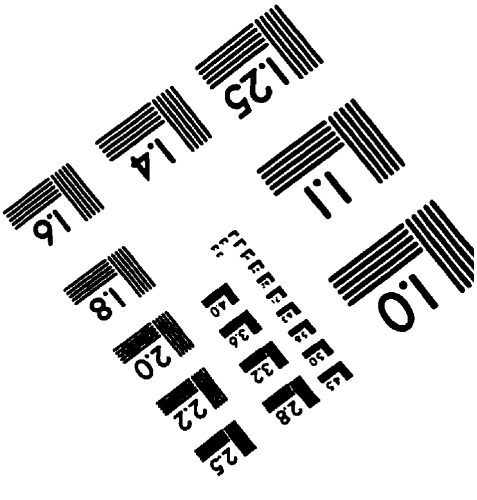

APPLIED IMAGE, Inc
1653 East Main Street
Rochester, NY 14609 USA
Phone: 716/482-0300
Fax: 716/288-5989